AD-A085 154 DAYTON UNIV OH RESEARCH INST F/G 7/4
NON-AQUEOUS ELECTRODE RESEARCH.(U)
MAR 80 R G KEIL, J R HOENIGMAN, W E MODDEMAN F33615-77-C-3156
UNCLASSIFIED UDR-TR-79-104 AFWAL-TR-80-2018 NL

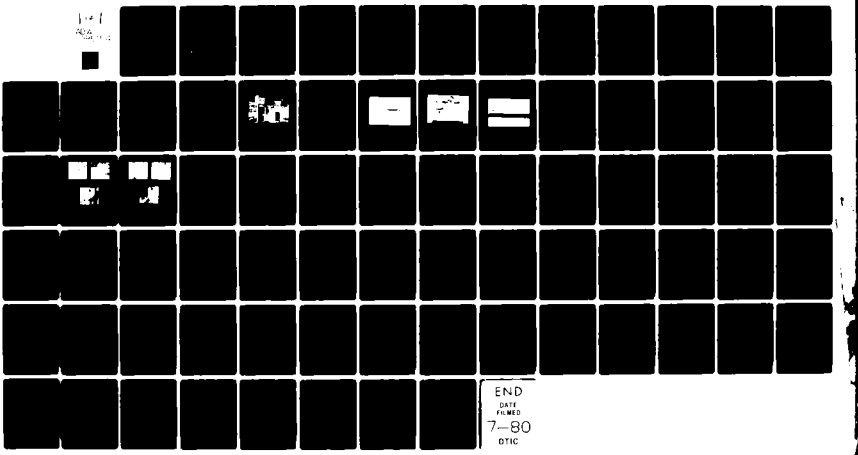

END
DATE FILMED
7-80
DTIC

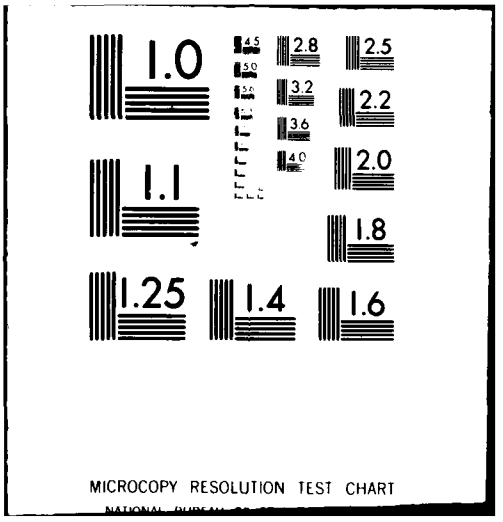
1.0
1.1
1.25
1.4
1.6
1.8
2.0
2.2
2.5
2.8
3.2
3.6
4.0
4.5
5.0
MICROCOPY RESOLUTION TEST CHART

LEVEL II

AFWAL-TR-80-2018

NON-AQUEOUS ELECTRODE RESEARCH

R. G. Keil
J. R. Hoenigman
W. E. Moddeman
T. N. Wittberg
J. A. Peters

March 1980

Technical Report AFWAL-TR-80-2018
Interim Technical Report: 1 October 1978 - 25 October 1979

Approved for public release; distribution unlimited

AERO PROPULSION LABORATORY
AIR FORCE WRIGHT AERONAUTICAL LABORATORIES
AIR FORCE SYSTEMS COMMAND
WRIGHT-PATTERSON AIR FORCE BASE, OHIO 45433

NOTICE

When Government drawings, specifications, or other data are used for any purpose other than in connection with a definitely related Government procurement operation, the United States Government thereby incurs no responsibility nor any obligation whatsoever; and the fact that the government may have formulated, furnished, or in any way supplied the said drawings, specifications, or other data, is not to be regarded by implication or otherwise as in any manner licensing the holder or any other person or corporation, or conveying any rights or permission to manufacture use, or sell any patented invention that may in any way be related thereto.

This report has been reviewed by the Office of Public Affairs (ASD/PA) and is releasable to the National Technical Information Service (NTIS). At NTIS, it will be available to the general public, including foreign nations.

This technical report has been reviewed and is approved for publication.

Robert L Kerr

R. L. KERR
Project Engineer
Energy Conversion Branch

FOR THE COMMANDER

James D. Reams

JAMES D. REAMS
Chief, Aerospace Power Division
Aero Propulsion Laboratory

"If your address has changed, if you wish to be removed from our mailing list, or if the addressee is no longer employed by your organization please notify AFWAL/POOC, W-PAFB, OH 45433 to help us maintain a current mailing list".

Copies of this report should not be returned unless return is required by security considerations, contractual obligations, or notice on a specific document.

SECURITY CLASSIFICATION OF THIS PAGE (When Data Entered)

REPORT DOCUMENTATION PAGE

READ INSTRUCTIONS BEFORE COMPLETING FORM

1. REPORT NUMBER: AFWAL-TR-80-2018	2. GOVT ACCESSION NO.: AD-A085154
3. RECIPIENT'S CATALOG NUMBER:	
4. TITLE (and Subtitle): NON-AQUEOUS ELECTRODE RESEARCH	5. TYPE OF REPORT & PERIOD COVERED: Interim Technical Report, 1 Oct 78 — 25 Oct 79
6. PERFORMING ORG. REPORT NUMBER: UDR-TR-79-104	
7. AUTHOR(s): R. G. Keil J. R. Hoenigman W. E. Moddeman T. N. Wittberg and J. A. Peters	8. CONTRACT OR GRANT NUMBER(s): F33615-77-C-3156
9. PERFORMING ORGANIZATION NAME AND ADDRESS: University of Dayton Research Institute, 300 College Park, Dayton, OH 45469	10. PROGRAM ELEMENT, PROJECT, TASK AREA & WORK UNIT NUMBERS: FY1455-79-00043, FY1455-79-00107
11. CONTROLLING OFFICE NAME AND ADDRESS: Aero Propulsion Laboratory AFWAL/POOC, AF Wright Aeronautical Laboratories, AFSC, Wright-Patterson Air Force Base, OH 45433	12. REPORT DATE: March 1980; 13. NUMBER OF PAGES: 78
14. MONITORING AGENCY NAME & ADDRESS (if different from Controlling Office)	15. SECURITY CLASS. (of this report): Unclassified; 15a. DECLASSIFICATION/DOWNGRADING SCHEDULE

16. DISTRIBUTION STATEMENT (of this Report)

Approved for public release; distribution unlimited

17. DISTRIBUTION STATEMENT (of the abstract entered in Block 20, if different from Report)

18. SUPPLEMENTARY NOTES

19. KEY WORDS (Continue on reverse side if necessary and identify by block number)

Batteries
Non-aqueous electrodes
Lithium anode
Thionyl chloride
Passive films
Scanning electron microscopy
X-ray photoelectron spectroscopy
Auger electron spectroscopy

20. ABSTRACT (Continue on reverse side if necessary and identify by block number)

This report describes work carried out in the second 13 months of a 33 month contract to characterize the passive films formed on anodes commonly used in non-aqueous battery cells, and to identify cell reaction products formed at the carbon cathode commonly used in these cells.

DD FORM 1 JAN 73 1473

SECURITY CLASSIFICATION OF THIS PAGE (When Data Entered)

105402

FOREWORD

This report was prepared by the University of Dayton Research Institute under Air Force Contract No. F33615-77-C-3156. The work was administered under the direction of the Aerospace Power Division, Energy Conversion Branch, Aero Propulsion Laboratory, with Dr. D. H. Fritts acting as Contract Monitor. This work is a continuation of the work reported in the Interim Technical Report, AFAPL-TR-79-2003, "Non-Aqueous Electrode Research", by M. H. Froning, W. E. Moddeman, T. N. Wittberg, and D. J. David, February 1979.

The financial support of this work by the Aero Propulsion Laboratory (AFWAL/POOC) at Wright-Patterson Air Force Base is gratefully acknowledged (Air Force Contract No. F33615-77-C-3156).

Special thanks go to Dr. David Fritts of the Aero Propulsion Laboratory, Project Monitor. In addition, the authors appreciate the encouragement and technical support of the following individuals: Dr. Robert McDonald and Dr. Nicolai Marincic of GTE Laboratories, Waltham, MA; Dr. David Chau and Mr. Don Bartlett of the Honeywell Power Sources Center, Horsham, PA; and Mr. Hal Grady of Foote Mineral Company, Exton, PA.

An additional note of thanks for his contribution is given to Dr. William E. Moddeman, who is presently on a leave of absence to the Department of Energy Facility at Mound Laboratories, Miamisburg, OH.

This report covers work conducted from 1 October 1978 through 25 October 1979.

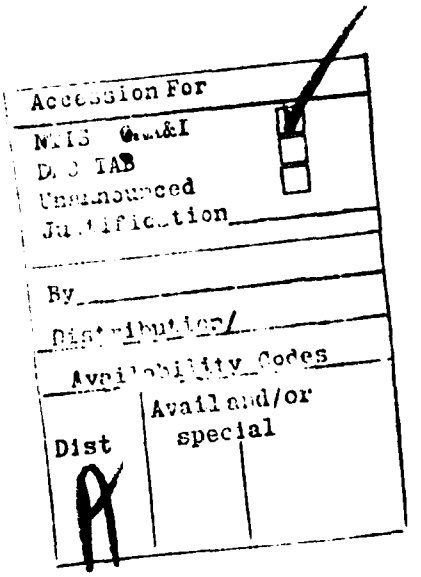

TABLE OF CONTENTS

LIST OF ILLUSTRATIONS

LIST OF ILLUSTRATIONS (CONTINUED)

LIST OF ILLUSTRATIONS (CONTINUED)

LIST OF ILLUSTRATIONS (CONCLUDED)

LIST OF TABLES

SECTION 1
INTRODUCTION

The basic constituents of a battery are a cathode, an anode, and an electrolyte which allows charge transfer to occur from the anode to the cathode. This arrangement is collectively re-referred to as a cell. A battery provides a potential difference and is capable of furnishing current for a period of time. In principle, any oxidation-reduction reaction can be used as a cell. Oxidation occurs at the anode and reduction occurs at the cathode.

From a theoretical standpoint, the anode and cathode materials which will provide the largest E.M.F. can be selected from a list of standard electrode potentials(1). Since the half cell E.M.F. of lithium is greatest of the metals, it immediately becomes a prime candidate as an anode material. In fact, the large E.M.F. that can be obtained, coupled with the possibility of high energy densities, (500 W-hr/kg) prompted interest in lithium batteries since the early 1960s.

Cathode reactions can be classified according to whether the cathode is in a solid or liquid physical state. The heavy metal halides, such as AgCl, $NiCl_2$, NiF_2, AgF, TiF_2, etc. received earliest attention because of their ability to be recharged (2,3). Consistent with their electrochemical reversibility, cells made with halide cathodes tend to have open circuit voltages close to their theoretical potential differences and are often capable of high rates of discharge. Unfortunately, high solubility of the halides results in cells of short life (2-4). Heavy metal sulfides and oxides are more insoluble than the halides and form cells of long life, but tend to provide only marginal cell capacity. Other materials proposed for cathodes include MnO_2 (5,6,7), V_2O_5 (8), MoO_3 (7,8,9,10), Ni_3S_2 (11), CuS (12), and recently Bi_2O_3 (13).

Insoluble cathode reactants may be obtained by treating graphite with fluorine (14). Depending on the experimental conditions, compounds with stochiometry close to $(C_4F)_n$, $(CF)_n$ may be obtained (15,16,17). The predicted voltages show these to be the most energetic materials yet proposed for use as cathode materials and the theoretical energy contents are impressively high. Unfortunately, the values obtained in use are much less, probably due to practical and other limitations which have not as yet been defined.

Further lithium battery development led Wilburn (18) to note that a primary lithium cell of long wet stand life and high discharge rate capability had finally emerged after more than a decade of activity in the area of high energy battery technology. These cells were based upon the use of a liquid cathode reactant such as SO_2 in an organic electrolyte (19) or an inorganic liquid cathode reactant (20,21,22). These systems are thought to passivate the lithium which is removed during cell discharge.

Auburn et al. (21) and Behl et al. (22) reported on cells utilizing oxyhalides with the addition of 1-2M $LiAlCl_4$ as an electrolyte and either graphite, carbon black or polycarbon monofluoride $(CF)_n$ as the cathode. Lithium was found to be stable in the three major oxyhalides studied (phosphorus oxytrichloride ($POCl_3$), sulfuryl chloride (SO_2Cl_2), and thionyl chloride ($SOCl_2$)). It was concluded from observations of the appearance of lithium anode surfaces, from cell performance, and from opinions based on the established reactivity of lithium that this stability was due to the formation of a passivation layer. Of course solvent reduction occurred during operation of the cell as a battery and energy densities in excess of 500W-hr/kg were reported (21). The thionyl chloride system showed the best performance compared to the other two oxyhalides due to its higher energy density even though the cell voltage of the SO_2Cl_2 system is higher than that of the $SOCl_2$ system (3.9V vs. 3.6V) respectively (23). These factors then prompted further investigation and development of the lithium thionyl chloride system.

One can propose many reactions and reaction products, consistent with a complex system, and favorable thermodynamic considerations. However, at this point in time, surface lithium reactions in a simple system are not understood. Thus, a priori, a study of the reactions of lithium surfaces will aid the understanding of the basic phenomena affecting battery performance.

Thionyl chloride is used as an electrolyte carrier and cathode depolarizer because of its ability to undergo electrochemical reduction. The continued development and investigation of primary lithium batteries based on $SOCl_2$ has highlighted three problems: 1) a voltage delay after storage at high temperature (24-28), 2) a tendency of the cells to explode at high rates of discharge, short circuit, or overdischarge (27), and 3) limited cell capacity based on the ability of the carbon cathode to accommodate products of reaction before passivation (23).

Approaches to alleviating the safety hazards associated with the use of these batteries have been investigated (29,30). It appears that the explosion problem is amenable to solution by providing for automatic venting, limiting the rate of discharge, and short circuit protection by the use of thermal fusing within the cell. The cathode limitation is being overcome by using a porous cathode with greater surface area while limiting the cell anode by controlling the quantity of lithium utilized (31).

The voltage delay phenomenon caused by passivation of the lithium surface has been studied by a number of workers (24-28,32). Driscoll et al. (32) reported that the voltage delay could be eliminated by pretreatment in 1.5M $LiAlCl_4/SOCl_2$ and that solution purity dramatically affected the voltage delay. Principal products of the discharge reaction were reported to be S, SO_2, and LiCl. Dey and Schlaikjer (26) examined the surface of lithium by SEM and energy dispersive x-ray analysis to characterize the passive film growth and its composition. These investigators concluded that the crystalline material on the lithium surface was LiCl.

In a separate study, Auburn et al. (21) concluded that the reaction products were mainly lithium chloride, sulfur, and lithium sulfite, while Holleck et al. (33) reported the reaction products to be lithium chloride, sulfur, and sulfur dioxide.

The three proposed reactions were then examined thermodynamically in an effort to determine if one of the calculated voltages compared more favorably to the measured open circuit voltage of approximately 3.6V. The free energy values of formation were obtained from Lattimer (1).

$$4Li + 2SOCl_2 \rightarrow 4LiCl + SO_2 + S, E^o = \frac{G^o}{-nF} = 3.688V$$

$$8Li + 3SOCl_2 \rightarrow 6LiCl + Li_2SO_3 + 2S, E^o = \frac{G^o}{-nF} = 3.574V$$

$$8Li + 4SOCl_2 \rightarrow Li_2S_2O_4 + 6LiCl + S_2Cl_2, E^o = \frac{G^o}{-nF} = 3.675V$$

Unfortunately, all of these values are within the experimental error of measurement so that no conclusion regarding the reaction can be reached based upon these calculations.

Chris et al. (28) have reported that film growth was observed only in the presence of $LiAlCl_4$ and the addition of 5% SO_2 reduces the voltage delay time.

In addition to the many complex reactions and factors that affect a lithium anode in a battery, the lithium must be fabricated into the proper anode configuration and in this process is exposed to environmental factors prior to its use in the battery.

It appears that a first step in attempting to understand the complex phenomena and reactions occurring within a primary lithium cell, is an understanding of the surface reactions of lithium with its environment before it is placed in the battery. It is obvious that the surface reaction products of lithium, passive or active, can influence the operation of the battery and perhaps provide insight to the proper handling of this material during anode processing and battery assembly.

Therefore, it is the purpose of this present study to investigate the surface reactions and passive film formation characteristics of lithium with its preassembly environment and the surface energetics and passive film formation properties of lithium with thionyl chloride, particularly in the initial stages of reaction.

SECTION 2
EQUIPMENT

1. DRY BOX

A dry box, obtained from Wright-Patterson Air Force Base, was transferred to the University of Dayton and refurbished to provide an environment where reactive and hazardous materials could be stored, reacted, and transferred for surface analysis with a minimum chance of contamination.

The major components of the system shown in Figure 1 are: 1) a provision for an inert atmosphere (Helium was used); 2) a recirculating pump for continual removal of any gaseous impurities such as water vapor from the helium, by pumping through molecular sieve columns; 3) a provision for a continuous helium positive pressure; 4) an isolation or transfer compartment which allows chemicals and equipment to be introduced into the box without contaminating the atmosphere with either air or water vapor; 5) a provision for regeneration of the molecular sieve; and 6) a relative humidity sensor for constant monitoring of the water vapor level in the dry box. A dewpoint of about $-78^{o}C$ (<2ppm H_2O) was maintained for the duration of this work.

2. XPS MODIFICATIONS

The original XPS vacuum system employed a combination of two oil diffusion pumps and a turbomolecular pump. This system proved to be inadequate for studying lithium metal. Contamination from the residual gases in the sample chamber, such as hydrocarbons and water, was a constant problem. These residual gases would react rapidly with a "freshly" created lithium metal surface. Thus, a "clean" lithium metal surface could not be characterized and gas/lithium metal exposure studies were impossible.

A new vacuum system was designed and constructed for the XPS instrument. This system is shown in Figure 2. Three types of vacuum pumps are used for evacuating the sample chamber. A

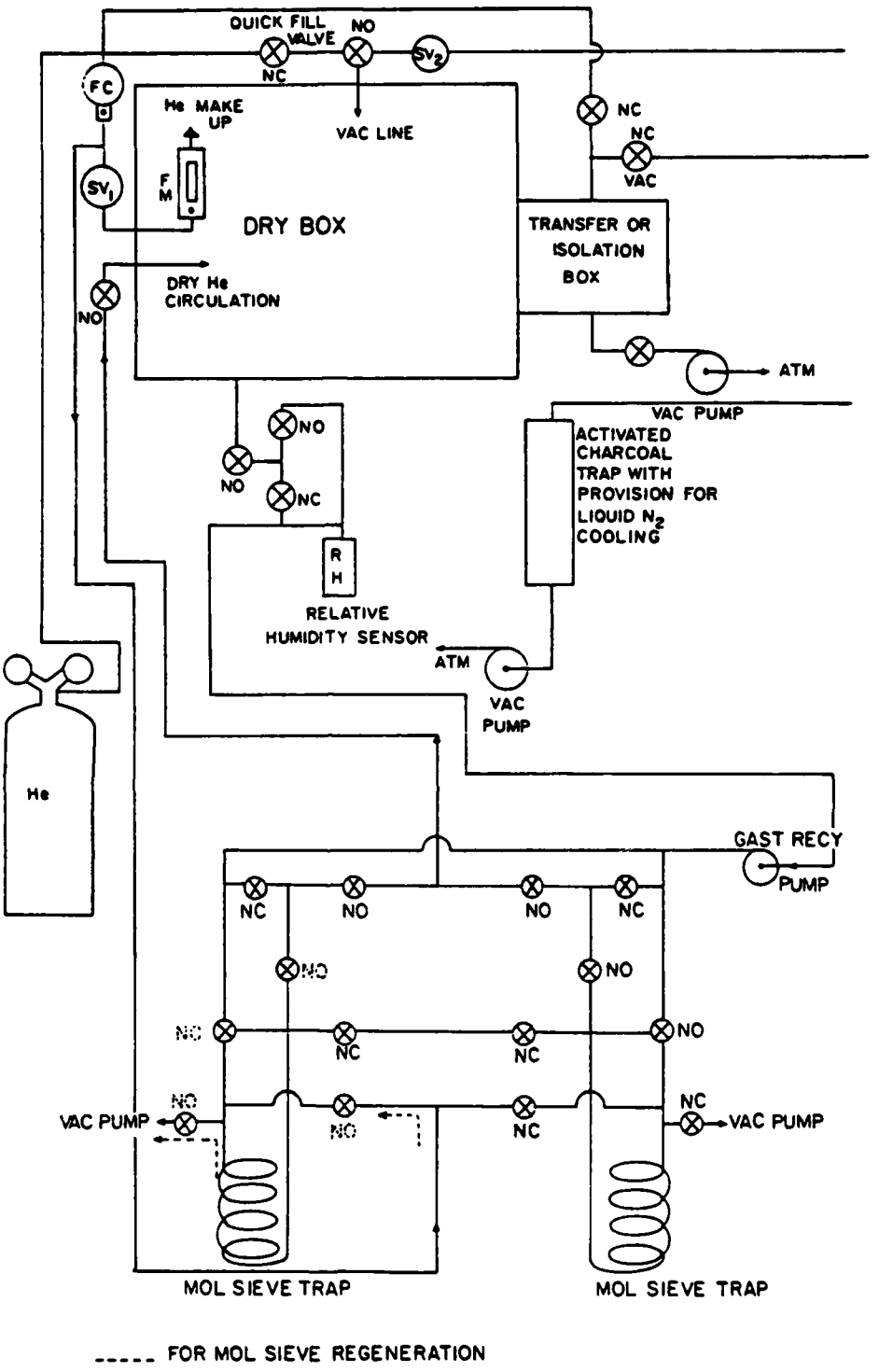

Figure 1. Block Diagram of Helium Dry Box and Purification System.

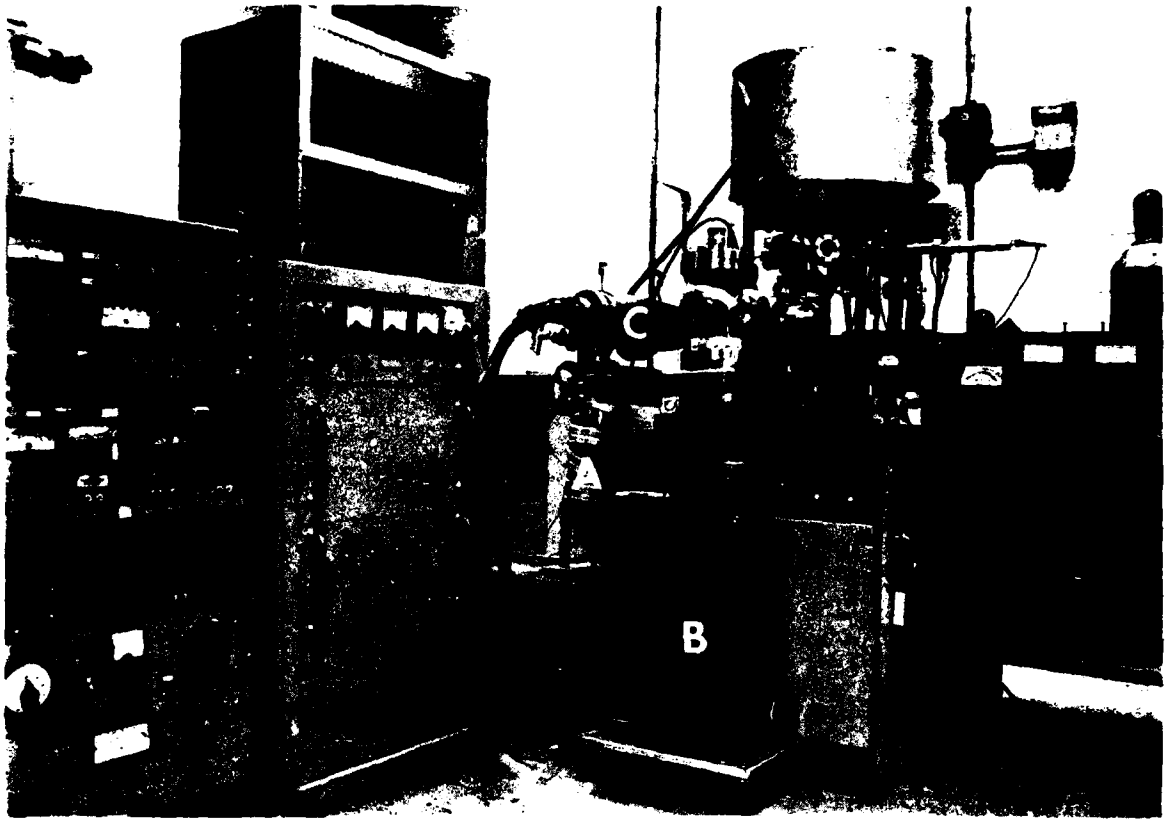

Figure 2. XPS System Showing the Redesigned Vacuum System.
A: Turbomolecular pump; B: Ion pump;
C: Titanium sublimation pump.

new turbomolecular pump (A in Figure 2) is the mainstay of the system. The turbomolecular pump is complemented by an ion pump (B in Figure 2) and a titanium sublimation pump (C in Figure 2). This system design allows simultaneous use of any desired combination of the three separate pumping systems. This design provides improved reliability and presents a clean environment for the analysis of lithium metal, and metal samples exposed to environmental gases.

3. SAMPLE HOLDER AND VACUUM INTERLOCK SYSTEM

A vacuum interlock system was designed for transferring lithium/$SOCl_2$ and battery anode samples from the helium dry box in which they are prepared into the XPS sample chamber for analysis. The two sections of the vacuum interlock system are shown in Figures 3 and 4. Figure 3 is the insertion stage, and Figure 4 is the transfer chamber. The corresponding sample holder for lithium metal is shown in Figure 5.

The vacuum interlock is composed of two sections which bolt onto opposite sides of the XPS sample chamber (Figures 3 and 4). On one side is a long .375 in. diameter stainless steel rod inside a stainless steel bellows (A in Figure 3). The rod can be rotated within the bellows via a vacuum rotary feedthrough (B in Figure 3). This rod is inserted through the XPS system into the sample transfer chamber. Utilizing the bellows and rotary feedthrough the rod is attached to the threaded end of the sample holder (D in Figure 5) and the sample is drawn into the XPS system. The other half of the interlock system is the actual transfer chamber (Figure 4). The transfer chamber consists of an ultrahigh vacuum gate valve (A in Figure 4), a sample chamber (B in Figure 4), and a viewing port (C in Figure 4). The transfer chamber is initially loaded with a sample inside the helium dry box. The gate valve is then closed and the transfer chamber is bolted onto the XPS unit. The use of a second

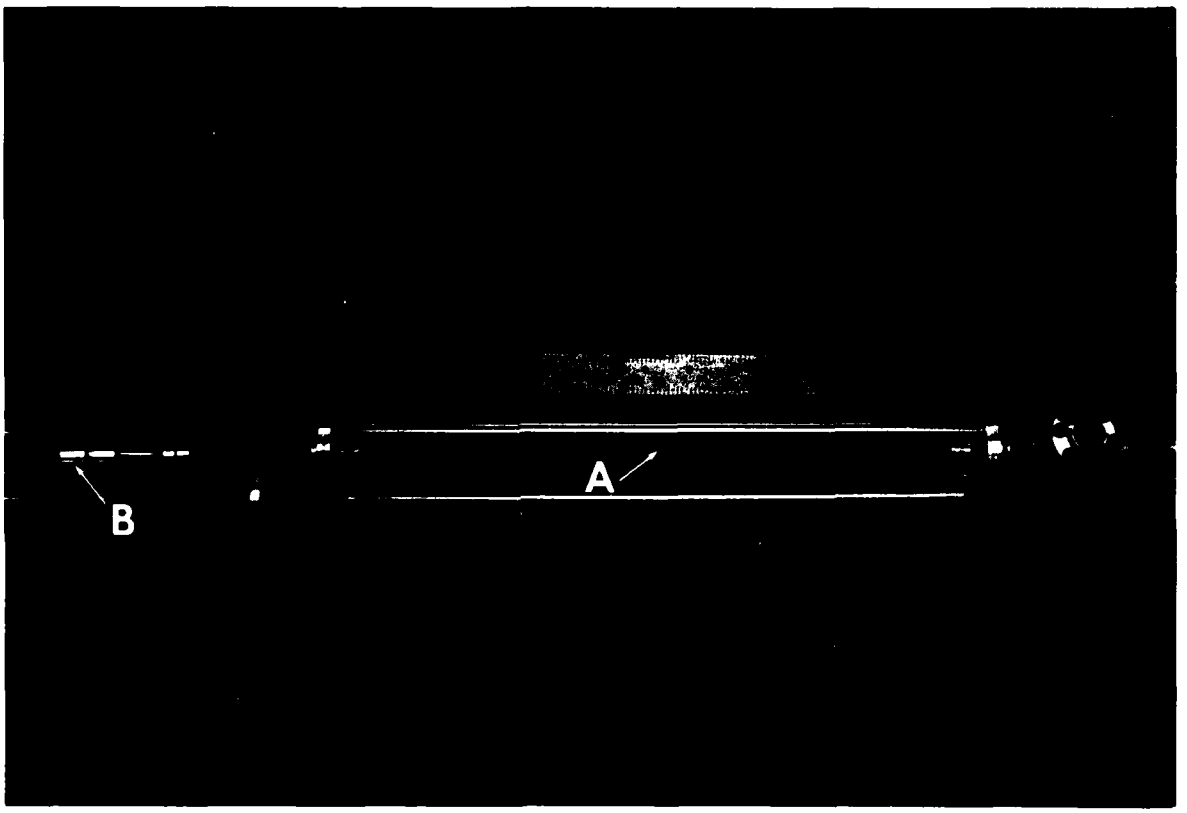

Figure 3. Sample Insertion Probe for the XPS System. A: Bellows assembly; B: Ultrahigh vacuum rotary feedthrough.

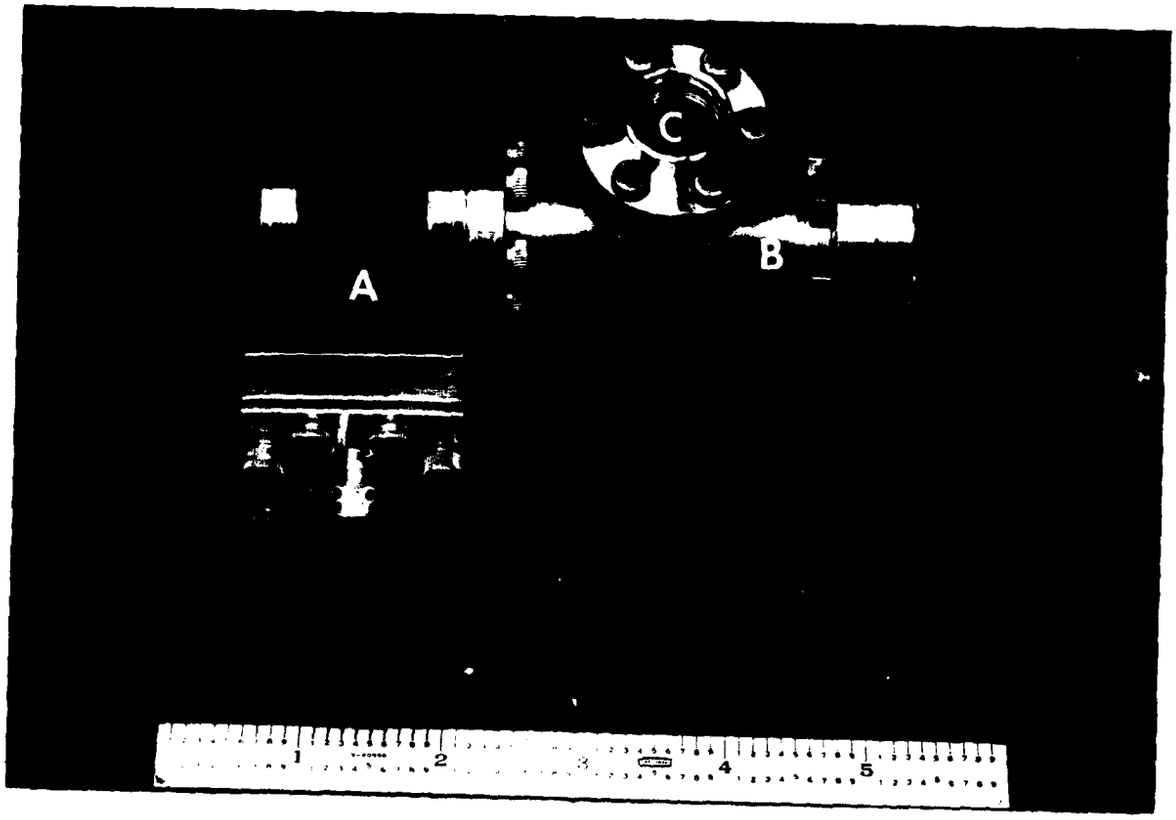

Figure 4. Lithium Sample Transfer Chamber. A: Ultrahigh vacuum gate valve; B: Sample chamber; C: Viewing port.

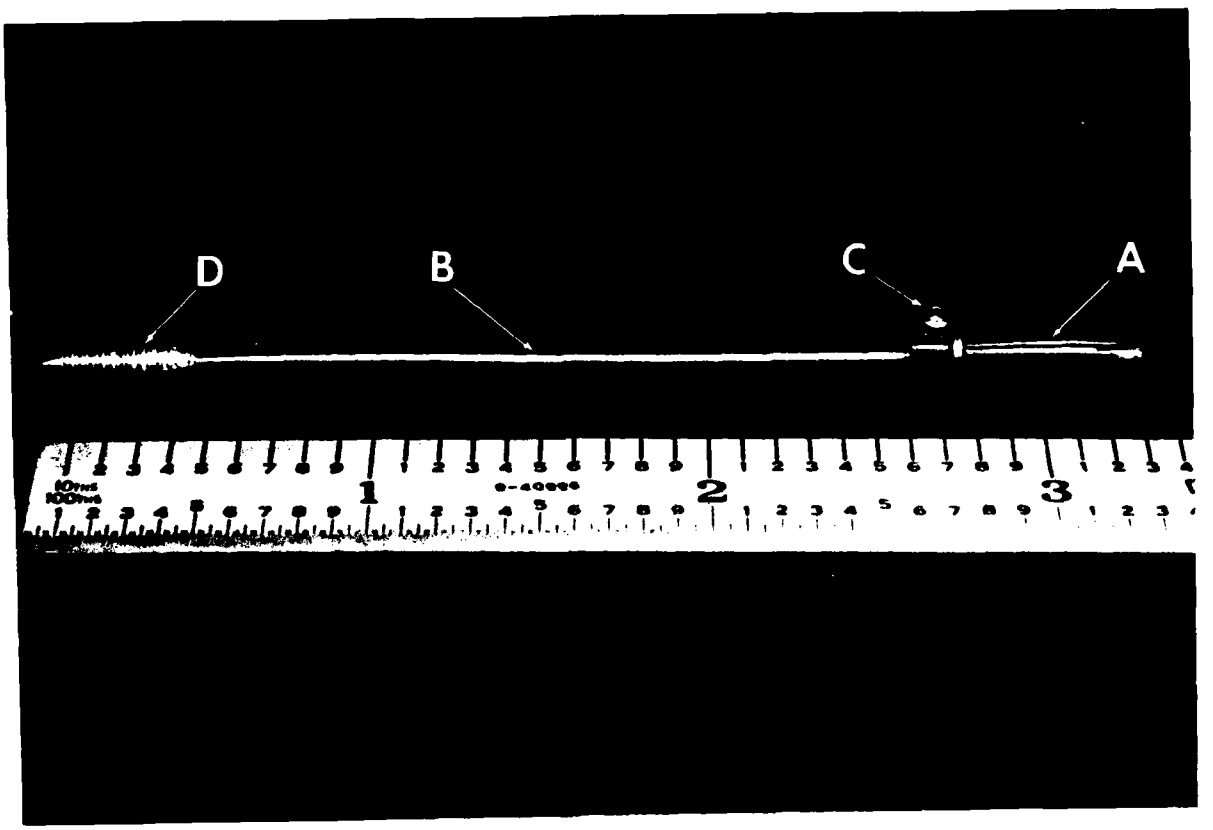

Figure 5. Lithium Sample Holder for the XPS System. A: Banana plug support; B: Sample rod; C: Set screw fastener; D: Threaded sample probe fastener.

gate valve on the XPS system permits simultaneous isolation of both the XPS system and the transfer chamber from atmosphere. Through the use of an additional valve the transfer system is evacuated using the turbomolecular pump. The sample is then pulled into the XPS chamber. This transfer system will be extensively utilized in all the XPS studies of lithium anodes.

The sample holder functions as follows: one end of the holder is composed of a standard banana plug (A in Figure 5). The banana plug is connected to a rod (B in Figure 5) by means of a small set screw (C in Figure 5). The opposite end of the sample holder is threaded (D in Figure 5). A sample of the lithium metal will be "speared" onto the holder rod such that the end faces of the lithium run parallel to the rod. The banana plug is then fastened on the rod. The banana plug will then be inserted into a hole in the end plate of the vacuum interlock. Once the interlock system is attached to the XPS instrument and evacuated, the sample will be pulled into the analysis chamber by screwing the insertion rod onto the threaded end of the sample holder and withdrawing the holder from the vacuum interlock.

4. GAS MANIFOLD SYSTEM

A separate system for the exposure of lithium to different gases was constructed. The gas manifold system shown in Figure 6 is composed of a central manifold with four gas cylinders connected in parallel. An ultrahigh vacuum flange on each end of the manifold allows the manifold to be connected to the Auger spectrometer and to a portable high vacuum system simultaneously. When this system was connected to the spectrometer gases of interest were introduced for direct reaction with the sample in the analysis chamber. In addition, the system will allow mixed gas reactions and sequential gas exposures to be carried out should this be desired.

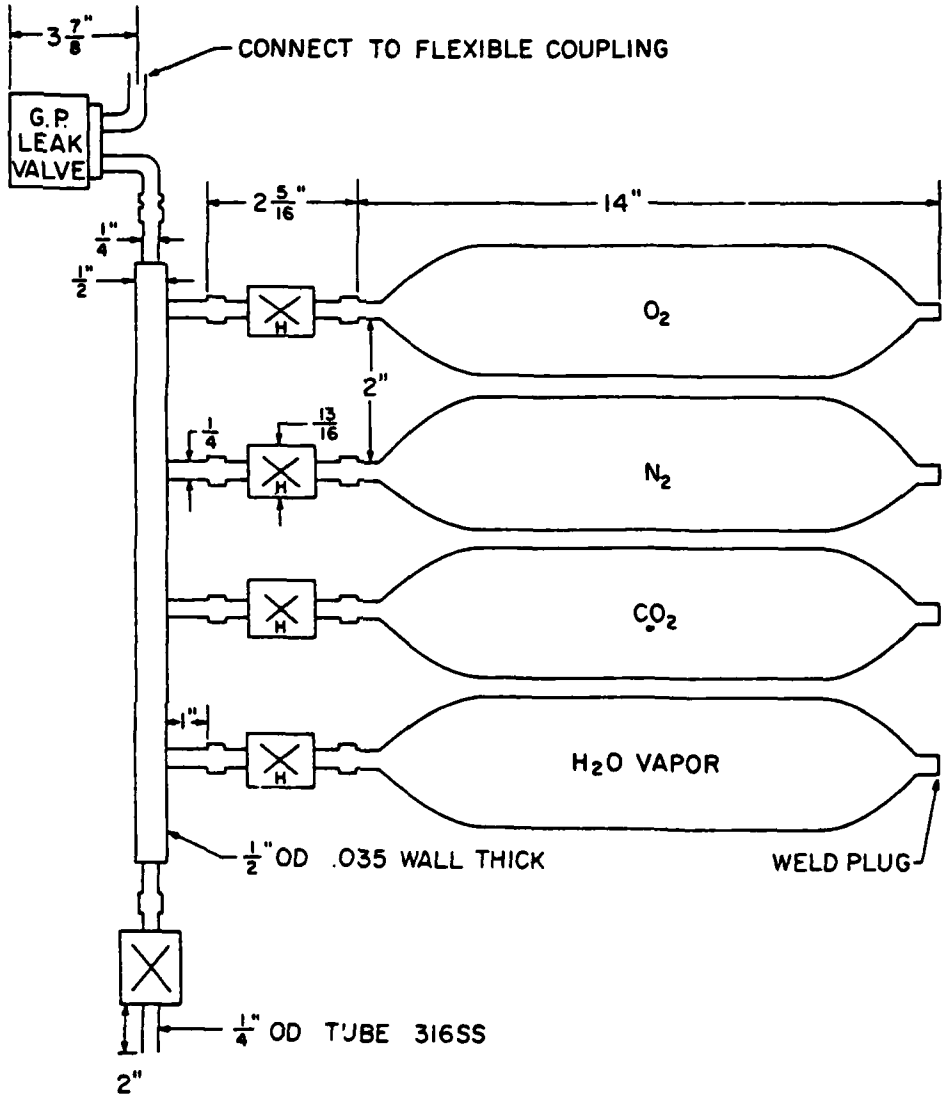

Figure 6. Gas Manifold for Vapor Exposure Studies on "Fresh" Lithium Surfaces.

5. CHEMICALS

Lithium

Lithium metal (99.9+%) supplied by GTE-Sylvania of Waltham, Massachusetts, consisted of pieces of ribbon approximately 0.3 cm x 0.5 cm x 6 cm sealed with sealing wax in screw-cap vials which had been blanketed with argon. High purity lithium was also obtained from Foote Mineral Company.

Thionyl Chloride

This material was supplied by GTE-Sylvania and was originally prepared by Mobay Chemical Company. The thionyl chloride was freshly distilled over lithium and was water white in appearance. Analysis by GTE-Sylvania showed less than 30 ppm of water in the $SOCl_2$. The analysis of the $SOCl_2$ is shown in Table I.

6. SAMPLE PREPARATION AND EXPOSURE

Materials as required were transferred to the dry box via a vacuum antechamber. A new, stainless steel, single edge razor blade was used to cut several small (0.5 cm x 1 cm) lithium samples from the as-received ribbons. These were then placed in a series of teflon lined screw cap septum vials along with approximately 15 ml of $SOCl_2$. The vials were stored in the dry box and samples removed at appropriate intervals for SEM or spectroscopic analysis.

Lithium samples were prepared for SEM examination as follows: individual samples were mounted on one inch diameter aluminum mounts using an electrically conductive silver-containing paint as a glue. Samples were positioned so that both a cut and an as-received surface could be observed. Samples were then transferred from the dry box to the SEM room in zip-lock polyethylene bags so as to minimize atmospheric contamination during transfer. In some cases, prior to SEM analysis a sputtered coating of Au/Pd was applied to the samples to eliminate charging effects and to improve the SEM image.

TABLE I

THIONYL CHLORIDE COMPOSITION

	Weight %
Component	Typical
Sulfuryl Chloride	<0.009%
Sulfur Chlorides	<0.1%
Sulfur Dioxide	<0.3%
Residue On Evaporation	<0.1%
Nickel	5 ppm
Iron	5 ppm
Lead	5 ppm
Copper	1 ppm
Zinc	1 ppm
Other Metals	10 ppm
Water	<50 ppm
Organics	Not Detected

Samples for analysis by Auger spectroscopy were prepared using the dry box described previously and were transferred to a plastic glove bag inflated with argon which was attached to the spectrometer entry port. The exact details of sample handling are discussed in the results section since they are important in understanding and interpreting the data.

SECTION 3
SCANNING ELECTRON MICROSCOPY

Upon examination of lithium anode samples which had been pretreated by storage in the battery assembly room at GTE-Sylvania for 88 hours, black spots were observed. The presence of the spots was unanticipated. The spots, approximately 200μm in diameter, were hemispherical and sharply defined. A particular feature that could be noted was the different surface appearance across the interface between the black spot and surrounding region (see Figure 7c). The spotted area appeared to be much smoother than the surrounding area.

The "as-received surfaces" of lithium that had been stored in GTE's argon dry box were of similar appearance, as the SEM photomicrographs in Figure 8 show. Dark spots were observed on the sample but were in general smaller and reduced in number by approximately one fourth. The surface textures were similar to those in Figure 7 but appeared to exhibit a slightly rougher texture. Similar results were observed for "freshly" cut lithium exposed to the GTE assembly room storage and those receiving argon inert atmosphere exposure.

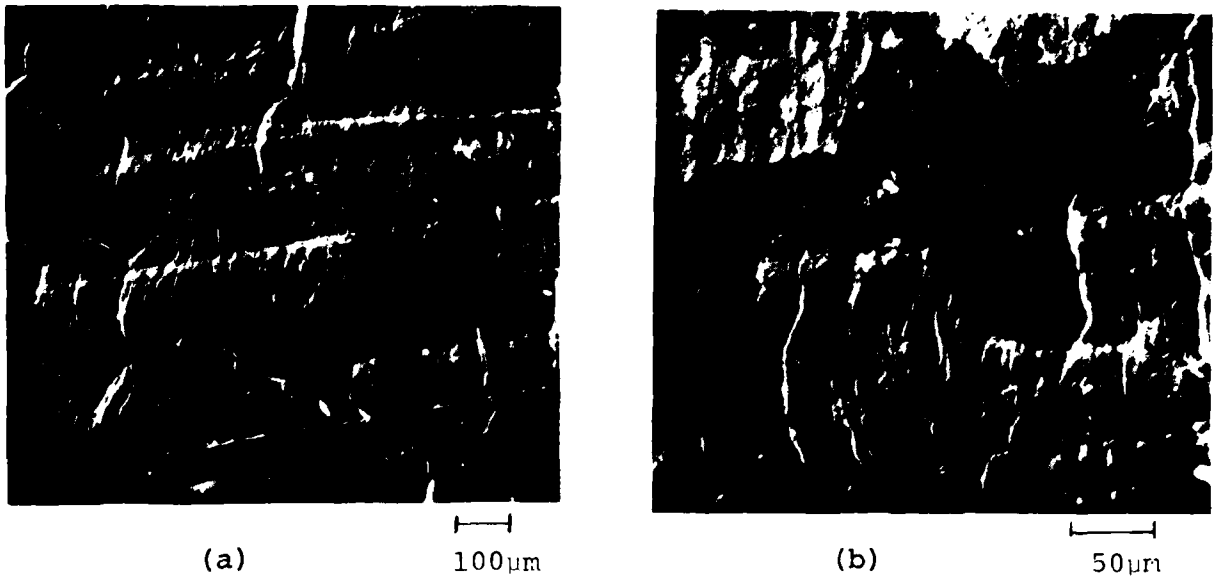

Figure 7. SEM Photomicrographs of an "As-Received" Lithium Metal Surface that was Exposed to the GTE-Sylvania Battery Assembly Room.

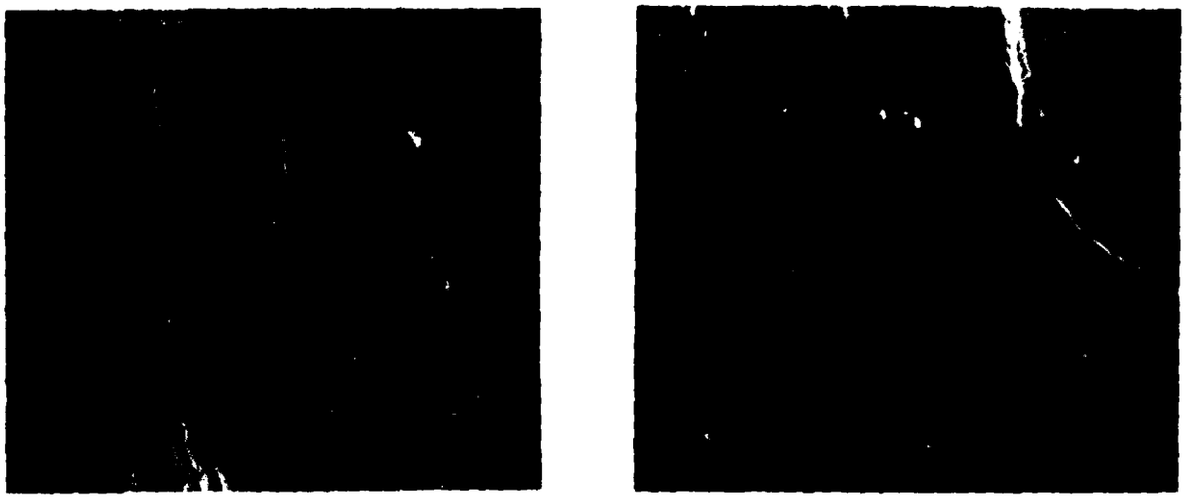

(a) (b)

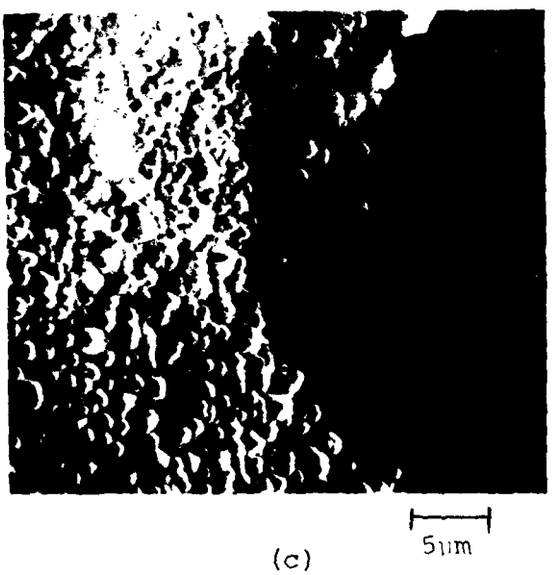

(c)
Black spot (right side)

Figure 8. SEM Photomicrographs of an "As-Received" Lithium Metal Surface that was Exposed to the GTE-Sylvania Laboratory Argon Dry Box.

SECTION 4
AUGER ELECTRON SPECTROSCOPY STUDIES

1. LITHIUM REACTIVITY WITH GASES

Initially samples were transferred to a portable glove bag which had been attached to the entry port of the Auger spectrometer. This bag was continuously purged and flushed with argon. "Freshly cut" lithium surfaces were prepared using a stainless steel razor blade. These samples were then loaded onto a sample tray and inserted into the spectrometer. The amount of oxygen detected using this technique was surprisingly large as evidenced by the large oxygen peak (509 eV) and the small lithium peak (50 eV). Sputtering at a high rate (15 mA at 3 kV) failed to remove substantial oxygen.

A significant improvement in transferring lithium samples resulting in slight oxygen contamination was achieved by immersing lithium samples in n-hexane.

Using the portable glove bag constructed around the entry port of the spectrometer, the samples were loaded as described previously with the exception that the samples were scraped/cut under n-hexane in a petri dish for protection from air and other gas reactions while they were loaded into the AES vacuum chamber. This technique proved successful in that oxygen and carbon peaks, although initially strong, were easily reduced by ion sputtering. It appears that the reaction of a fresh lithium surface with n-hexane provides a passive film which retards further reactions, including heavy oxide formation, for some period of time. Figure 9 shows the native surface while Figure 10 presents the same surface after about 10 minutes sputtering. Figure 11 shows the depth profile as a function of time for the n-hexane passivated surface.

For exposure studies, fresh lithium surfaces were cut under n-hexane in the glove bag and inserted into the instrument as described previously. To calibrate for instrumental contamination the sample chamber was evacuated to 10^{-9} Torr, the ion pumps were

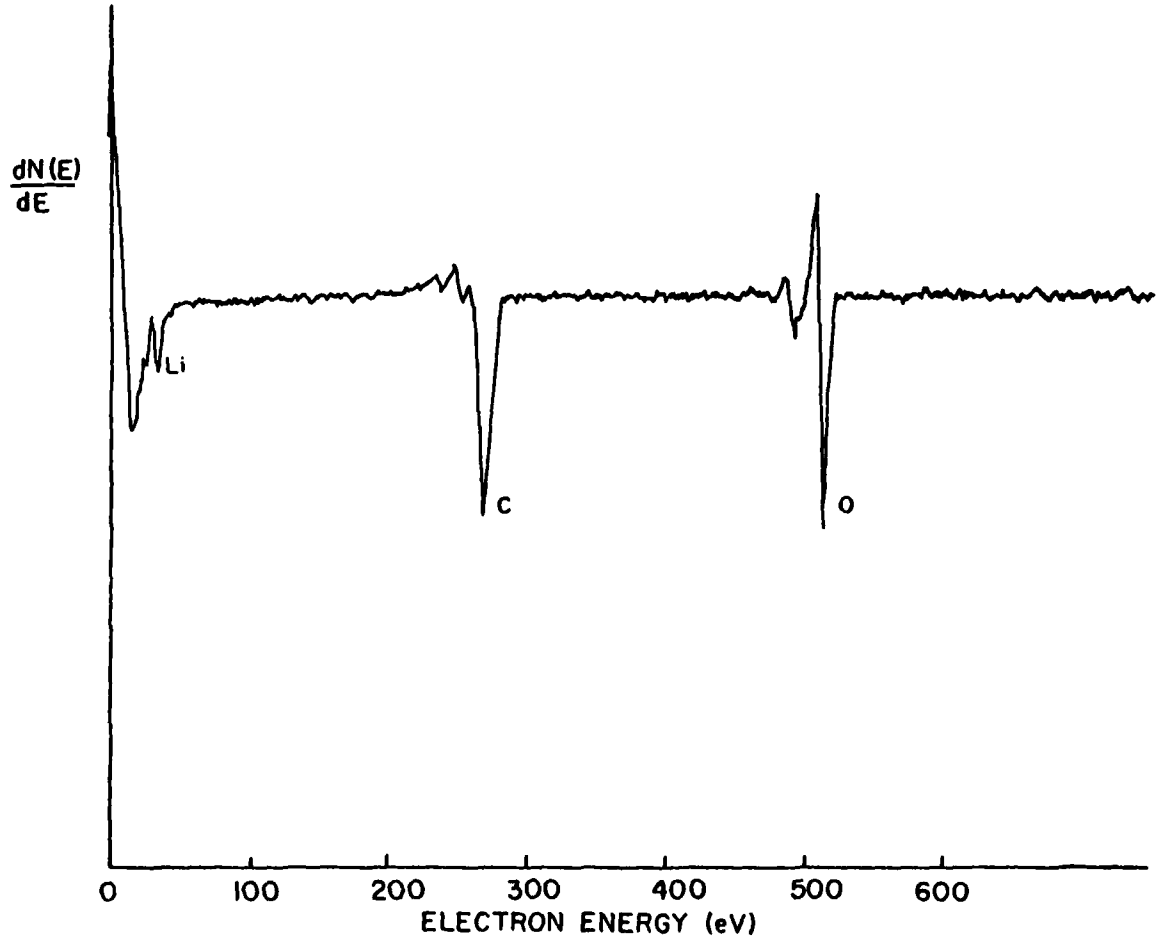

Figure 9. Auger Spectrum of Lithium Surface "Freshly Cut" Under n-Hexane.

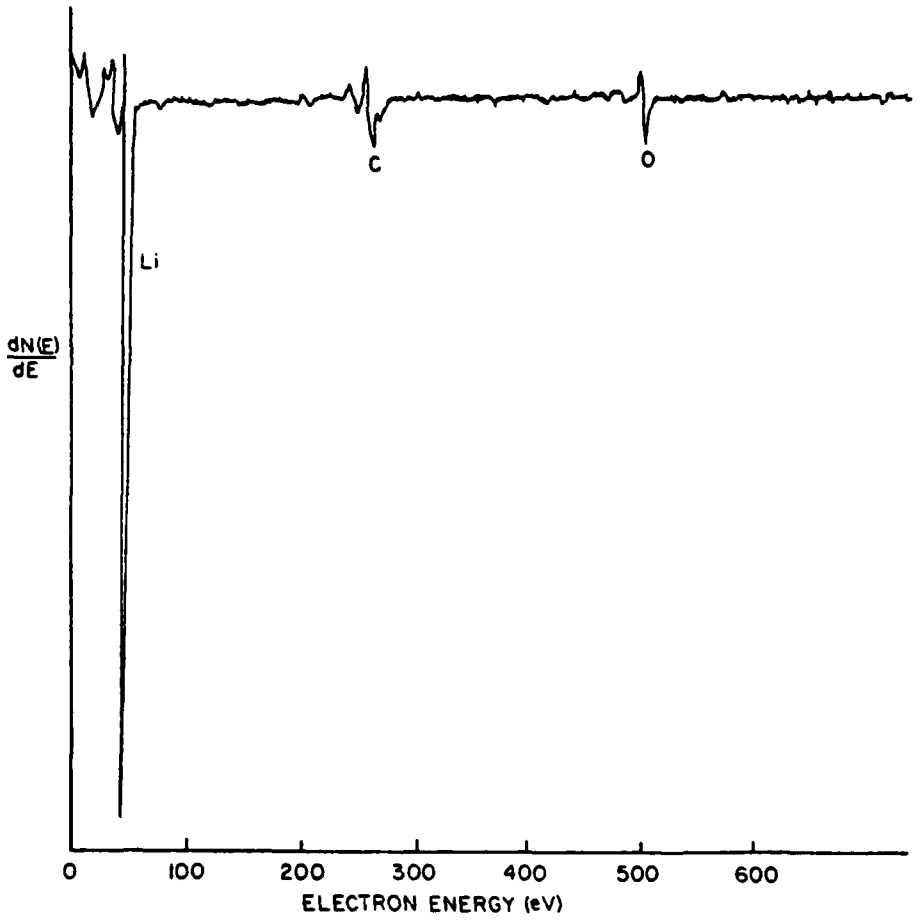

Figure 10. Auger Spectrum of Lithium Surface After 10 Minutes of Ion Sputtering. Sample was "Freshly Cut" Under n-Hexane.

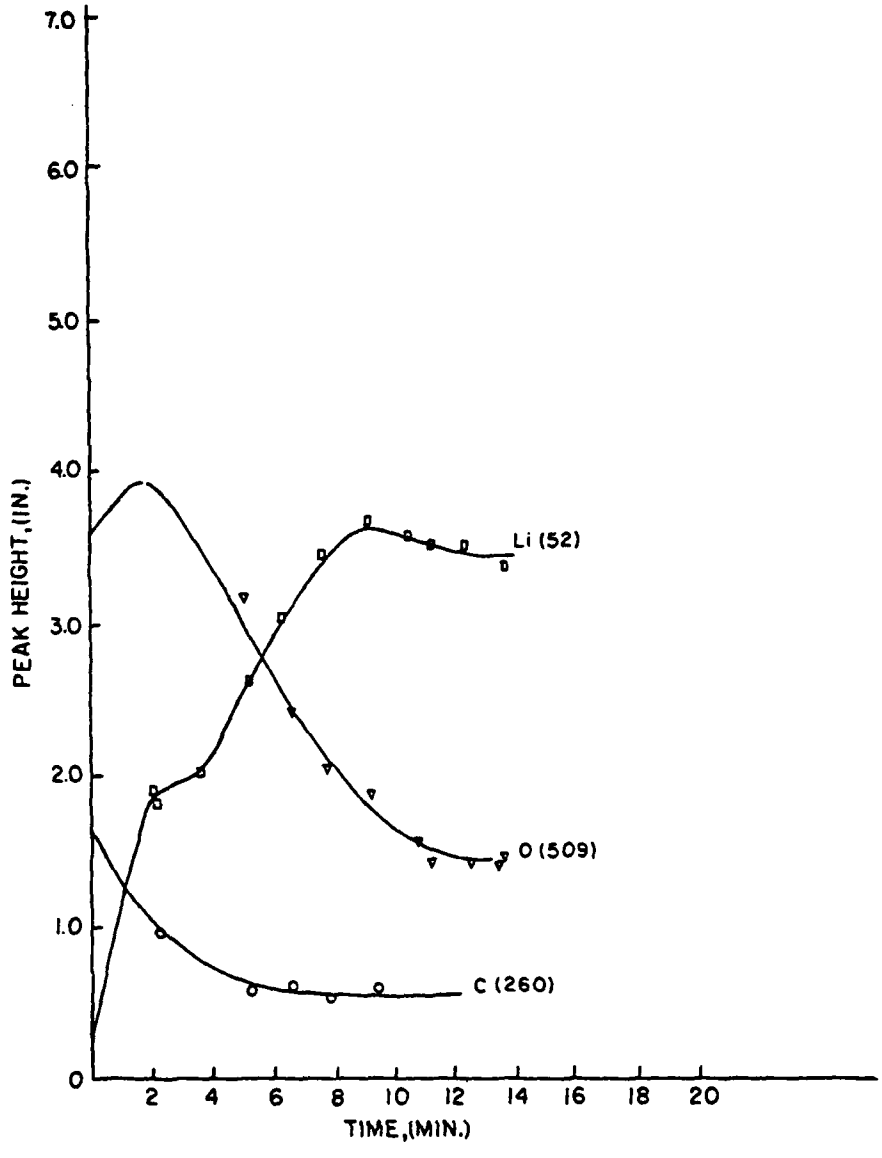

Figure 11. Auger Profile of Lithium Surface "Freshly Cut" Under n-Hexane.

closed off, argon was introduced, the sample was sputtered clean, and the chamber was again evacuated. With the ion pumps later turned off, spectra of lithium were taken periodically. If the surface cleanliness of the lithium was not maintained under these conditions the procedure was repeated until it was.

Controlled amounts of gases were introduced through a leak valve which was an integral part of the vacuum system. After selected periods of time at measured pressures, the chamber was evacuated and the sample was rescanned immediately. These data are shown in Table II and plotted in Figure 12 as appropriate ratios referenced to the metallic lithium peak.

It can be seen from Figure 12 that the reaction rate of lithium with nitrogen is the lowest of any of the gases utilized. To substantiate the slow reaction rate of lithium with nitrogen, the experiment was repeated by exposing lithium to nitrogen for long time periods without pumping down and sputtering between runs. This experiment confirmed the previous data, nitrogen was found to react very slowly.

Figures 13 and 14 illustrate the differences in the reaction rates of CO_2 and O_2. Scans both before and after exposure are included for comparison. For approximately the same exposure levels the Li-CO_2 exposed spectrum shows a decayed lithium peak (51eV) and a large (38eV) peak while the Li-O_2 exposed spectrum shows a practically unchanged lithium peak. These peak shifts indicate a change in oxidation state of a surface component, in this case lithium.

Although the Li-CO_2 exposed spectrum shows some evidence of carbonate formation judged by the increase in carbon (272eV) and the peak shape, these results were not consistent. After much higher CO_2 exposures the carbon peak did not increase and was approximately the same level as in the scan before CO_2 introduction (see Figure 15). However, the 38eV peak has increased to an apparent equilibrium value.

TABLE II

AUGER RESPONSE OF LITHIUM TO VARIOUS GASES

Gas	Exposure in Langmuirs	Response Ratios 38eV/Li	380eV/Li	509eV/Li
O_2	2.4×10^2	0.33	--	0.50
O_2	4.3×10^3	1.60	--	3.00
O_2	1.9×10^4	1.59	--	3.00
CO_2	4.6×10^2	0.80	--	1.36
CO_2	7.9×10^3	1.63	--	2.91
CO_2	1.9×10^4	1.84	--	3.05
N_2	3.0×10^3	--	--	--
N_2	4.7×10^5	--	0.37	1.58
N_2	5.0×10^6	--	0.58	1.80
N_2	1.1×10^7	--	0.68	1.80
H_2O	4.8	0.15	--	0.23
H_2O	4.8×10^3	0.17	--	0.28
H_2O	6.2×10^4	0.31	--	0.50
H_2O	9.2×10^5	0.75	--	1.50
H_2O	1.4×10^6	0.79	--	1.64

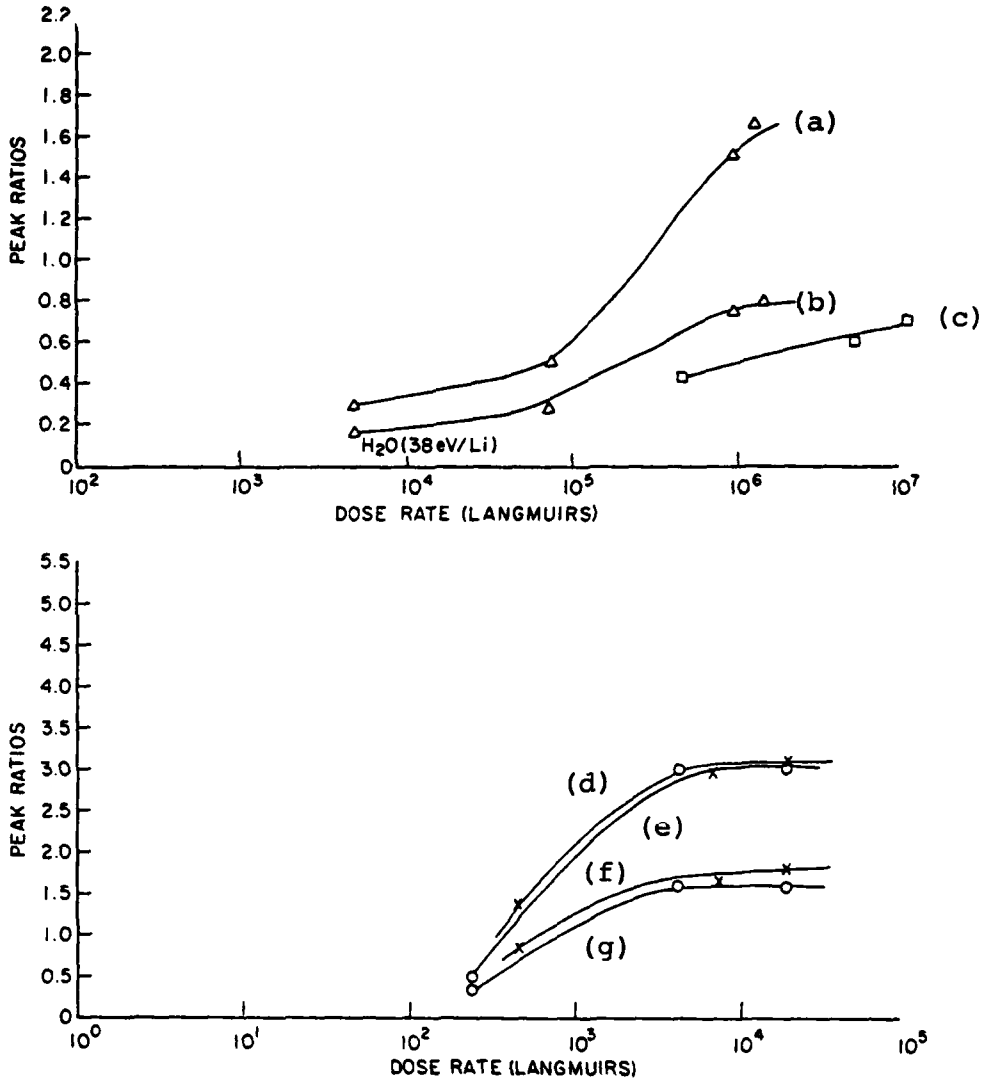

Figure 12. Relative Response Ratios of H_2O, N_2, CO_2, and O_2 versus Dose Rate. a) O (509eV)/Li(51eV) Auger peak ratios for H_2O exposures. b) Li(38eV)/Li(51eV) Auger peak ratios for H_2O exposures. c) N (380eV)/Li(51eV) Auger peak ratios for N_2 exposures. d) O (509eV)/Li(51eV) Auger peak ratios for CO_2 exposures. e) O (509eV)/Li(51eV) Auger peak ratios for O_2 exposures. f) Li (38eV)/Li(51eV) Auger peak ratios for CO_2 exposures. g) Li(38eV)/Li(51eV) Auger peak ratios for O_2 exposures.

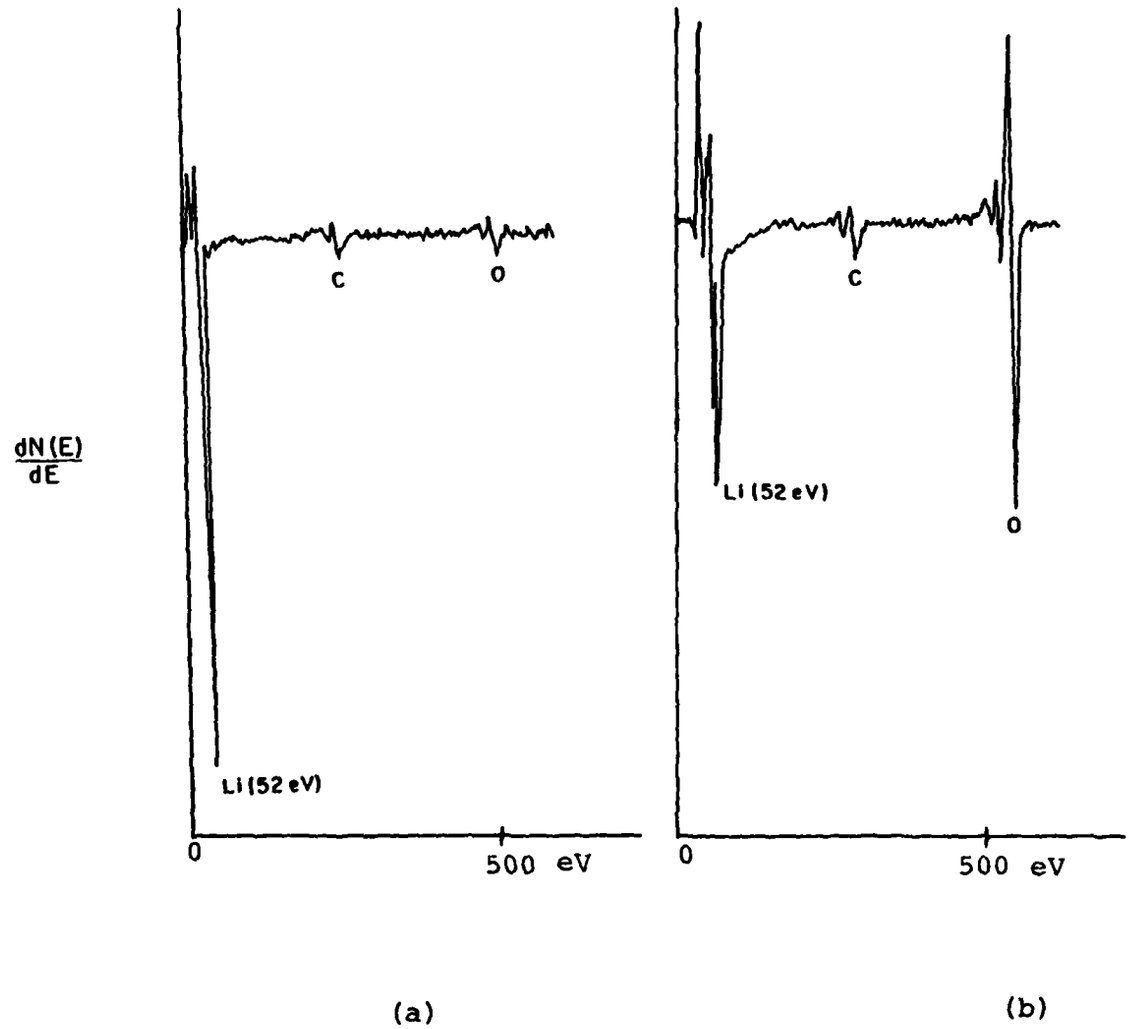

Figure 13. Auger Spectra of Lithium; a) Before Exposure; b) After Exposure to 4.6×10^2 Langmuirs of CO_2.

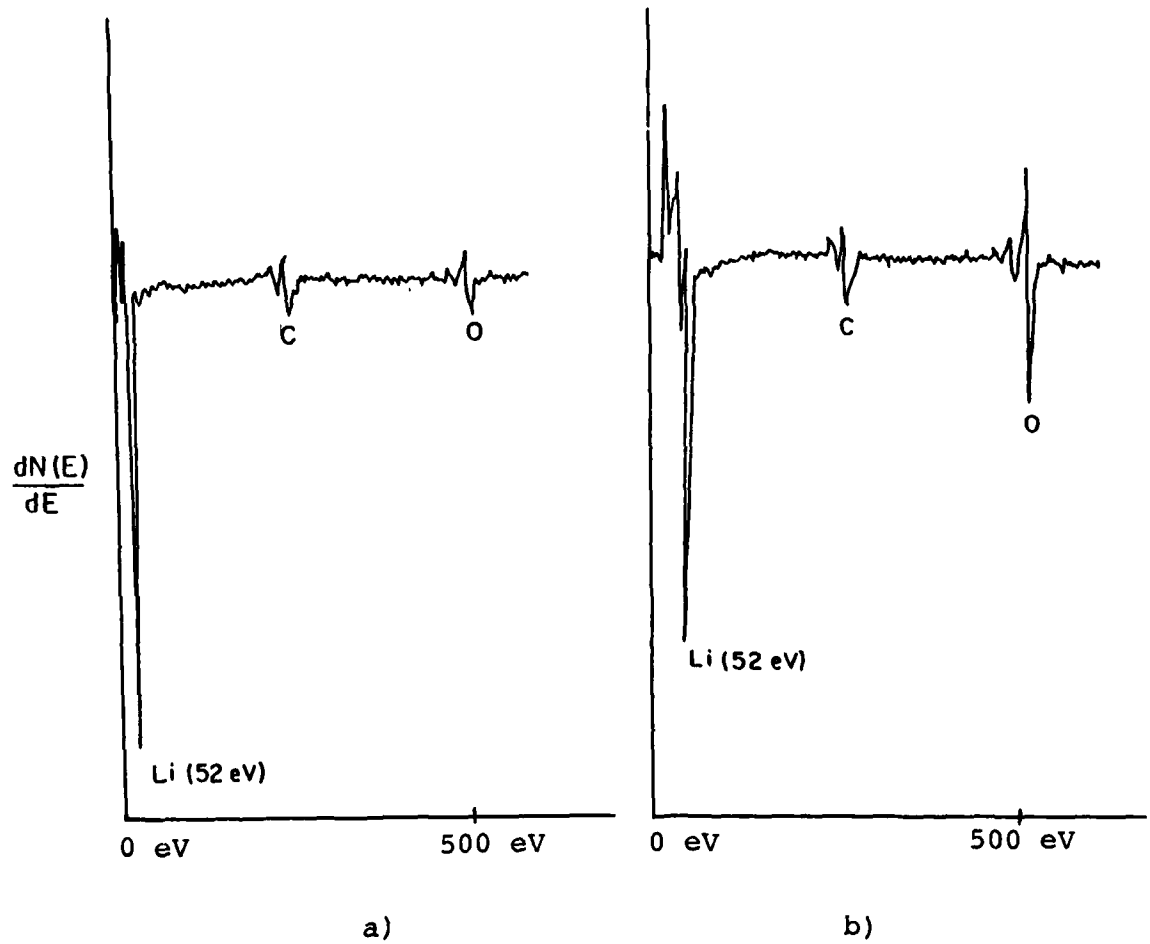

Figure 14. Auger Spectra of Lithium; a) Before Exposure; b) After Exposure to 2.4×10^2 Langmuirs of O_2.

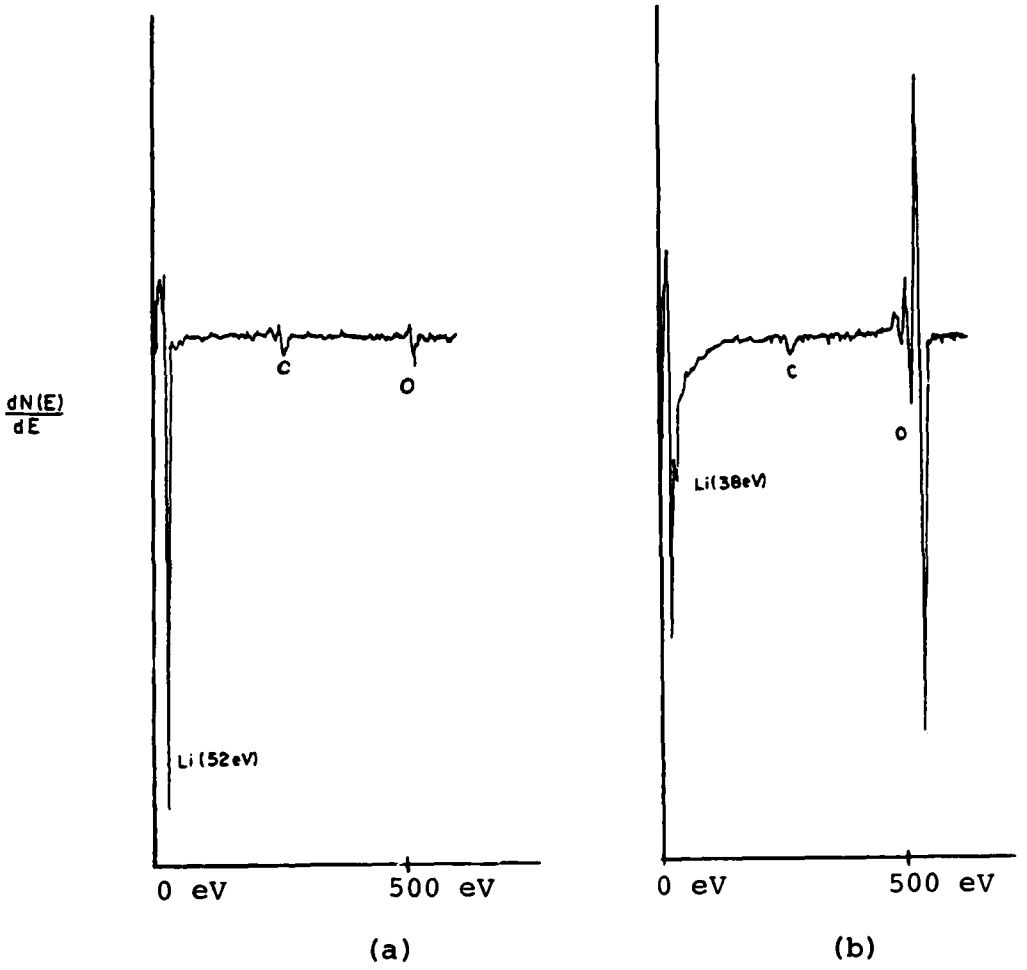

Figure 15. Auger Spectra of Lithium: a) Before Exposure; b) After Exposure to 1.9×10^4 Langmuirs of CO_2.

These data indicate that the major reaction might be $2Li + CO_2 \longrightarrow Li_2O + CO$. Another possibility for the observed results, which cannot be ruled out, is electron beam desorption or the decomposition of the carbonate in this case with the electron beam creating CO_2 as a result.

The faster reaction rate of CO_2 would not be anticipated on the basis of dissociation energies since the CO_2 energy is higher than that of O_2, 191 kcal/mole vs. 118 kcal/mole respectively. However, lithium is a very reactive material and should have some highly energetic surface sites.

The reaction with H_2O was found to be slow and even at the highest dose rate, unreacted lithium remained as shown in Figure 16. This scan indicates the presence of an oxide (hydroxide) since the (38eV) peak has remained relatively constant in size. At this point, CO_2 was introduced into the system since it was thought that perhaps to form the carbonate, hydroxide must be present initially and the reaction could proceed via

$$LiOH + CO_2 \longrightarrow LiHCO_3$$

$$LiHCO_3 + LiOH \longrightarrow Li_2CO_3 + H_2O$$

A dose rate of 9.2×10^4 Langmuirs H_2O was followed by a dose rate of 2.6×10^5 Langmuirs CO_2 and found to produce the same results. After CO_2 introduction and rescanning, an Auger spectrum was produced which was identical to the Li-CO_2 exposure spectrum. After one scan (1.5 minutes) the spectrum returned in appearance to that of the H_2O exposure spectrum before CO_2 introduction. This is shown in Figure 17.

This would indicate that the CO_2 probably does not react immediately with the hydroxide surface and may be merely physisorbed with the result that the electron beam immediately desorbs the CO_2. The initial 38eV/Li ratio of 2.03 and the 509eV/Li ratio of 2.98 compare favorably with that found in the Li-CO_2 reaction product (Table II). It should be noted that the carbon peak did not increase.

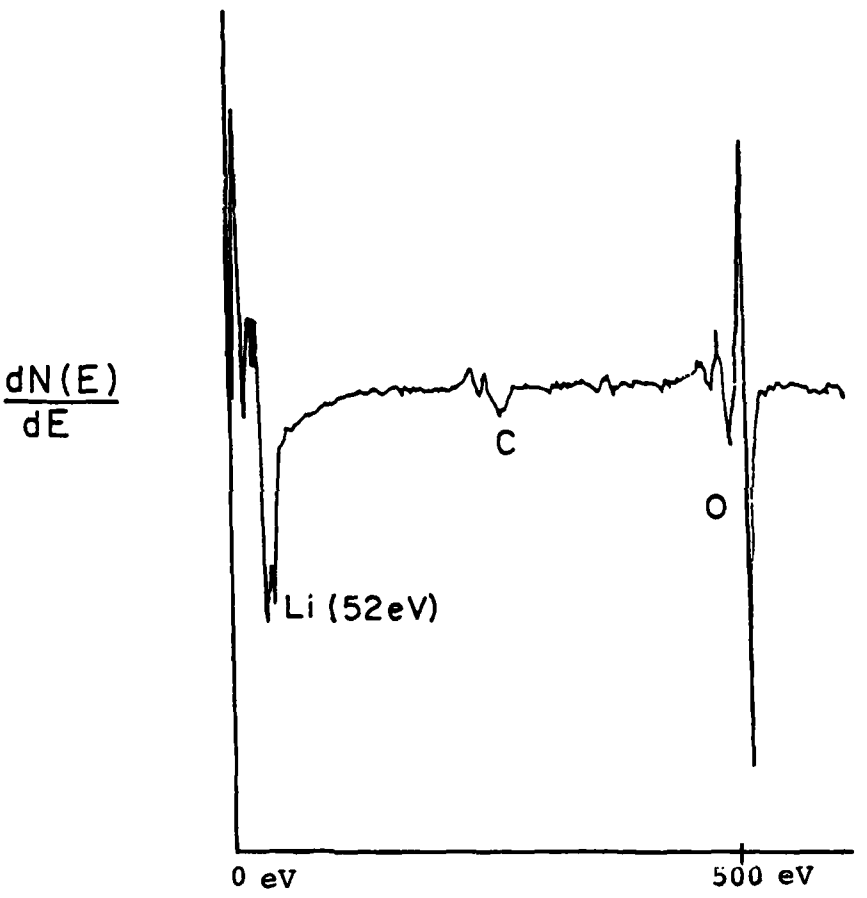

Figure 16. Auger Spectrum of Lithium Exposed to 1.4×10^6 Langmuirs of Water Vapor.

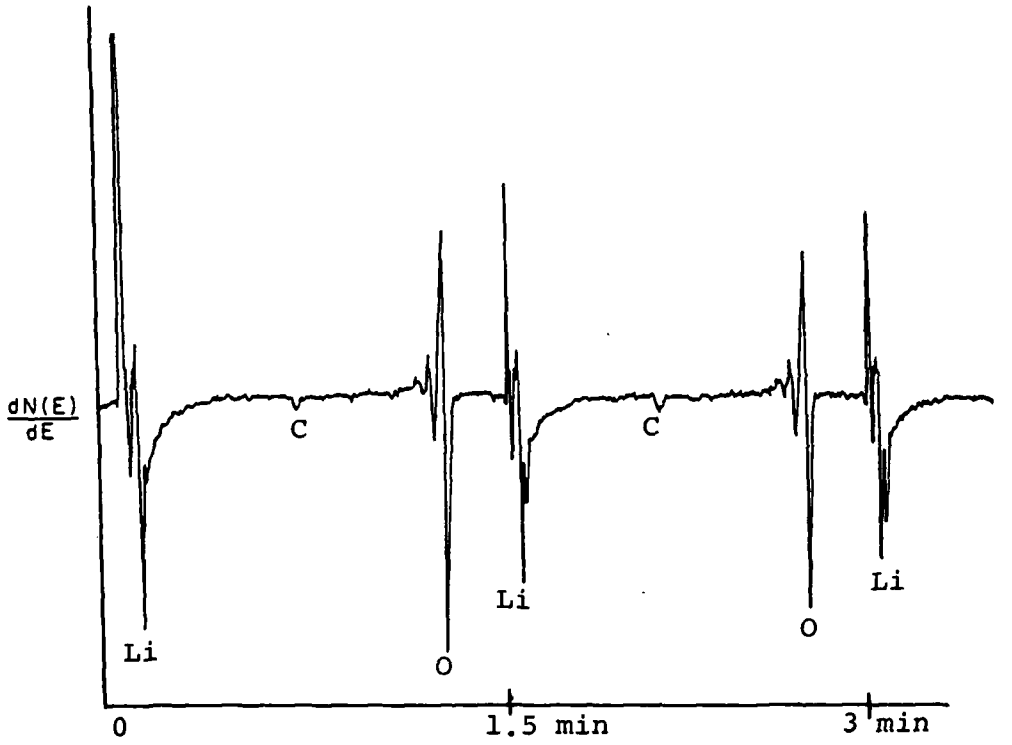

Figure 17. Auger Spectrum Demonstrating the Desorption of CO_2 from a Lithium Surface Having Had a Dual Exposure to 1.4×10^6 Langmuirs of H_2O Followed by 3.6×10^5 Langmuirs of CO_2.

2. THE PRODUCTION OF CLEAN LITHIUM SURFACES

A lithium preparation technique was previously reported,[34] whereby lithium was cut under n-hexane prior to insertion into the AES vacuum chamber. Apparently, the n-hexane results in formation of a relatively thin passive surface layer which acts as a barrier to lithium oxidation during transfer into the AES vacuum chamber. This passive layer is subsequently removed by ion sputtering to reveal the underlying lithium surface.

An example of our earlier reported[34] attempts at preparing a clean lithium surface is shown in Figure 18. A small amount of oxygen is still detectable on the lithium surface after 35 minutes of sputtering. Also, one should note a very weak carbon peak visible in the vicinity of 270 eV. These oxygen and carbon contamination levels could influence gas exposure test results. Thus, it was decided to further refine our sample cleaning technique so as to assure the integrity of future gas adsorption data.

In order to minimize oxygen contamination, an as-received lithium ribbon approximately 3 cm L x 1 cm W x 0.3 cm T was removed from its shipping carton inside a helium glove box ($\sim$ 1 ppm H_2O) and placed into a 25 ml glass vial with a teflon-lined rubber septum screw-on cap. The vial was tightly sealed while still in the dry helium atmosphere of the glove box and then the vial was passed outside of the box via the vacuum access port. Approximately 20 ml of n-hexane were then injected into the vial with a syringe. This procedure made it possible to completely immerse the lithium in n-hexane without removal from the dry helium atmosphere of the glove box. The septum vial was then transferred to a plastic glove bag which was attached to the AES vacuum chamber. Under a cover flow of argon gas, the following steps occurred: (1) the lithium in n-hexane was transferred to a large petri dish; (2) fresh surfaces were cut under the hexane; (3) these specimens were mounted on an aluminum AES sample tray; and (4) the sample tray was positioned into the AES chamber for analysis. The chamber was evacuated and baked overnight @ 100°C to attain a chamber vacuum of 3×10^{-10} Torr.

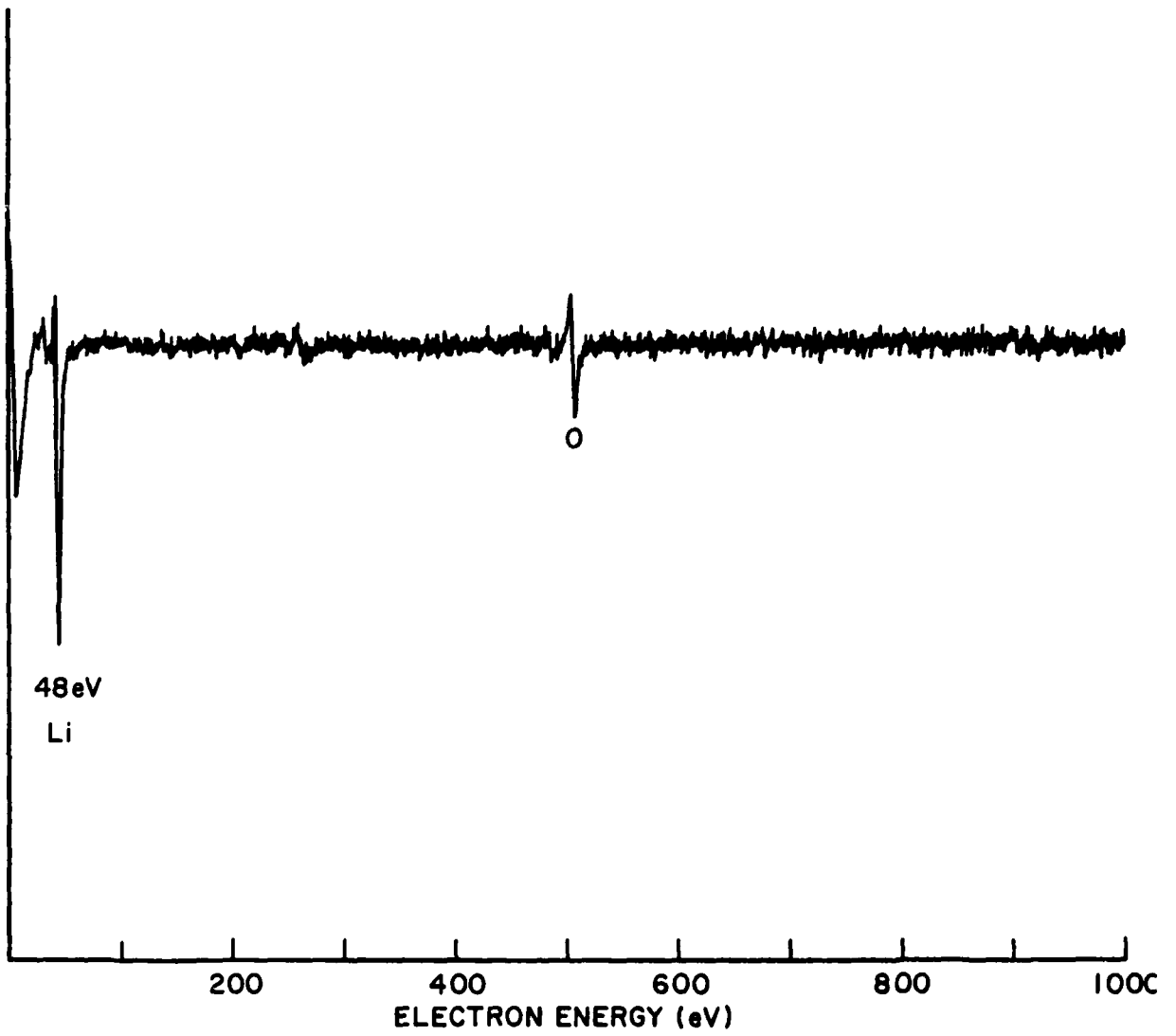

Figure 18. Auger Spectrum From an Early Attempt at Producing a "Clean" Lithium Metal Surface After 35 Minutes of Argon Ion Sputtering.

A lithium surface cut under n-hexane is shown in Figure 19. Contamination peaks of oxygen, carbon, chlorine, and nitrogen were found following the cutting and handling operations. After sputtering the exposed surface with an argon ion gun for 5 minutes operated at 3 kV and 10 mA electron emission current, only small oxygen and carbon peaks remained. This result is shown in Figure 20. After 17 minutes of sputtering (Figure 21), the oxygen and carbon peaks were reduced to near background levels. Additional sputtering did not further reduce the oxygen and carbon levels. However, a cleaner lithium spectrum was obtained by alternately argon ion sputtering and ion pumping the chamber several times. This procedure prevents contaminants from reacting with the freshly sputtered surface and eventually led to the clean surface spectrum shown in Figure 22.

Having established what was deemed to be an optimum lithium surface preparation procedure, an investigation was performed to determine the reactivity of this surface with the residual gases in the Auger vacuum chamber. Due to its high reactivity, a freshly sputtered lithium surface will act as a "getter" for any active residual gas in the chamber. After obtaining such a lithium surface, the argon was removed by the ion pumps. Under ultrahigh vacuum conditions the carbon and oxygen Auger peaks slowly increased and after 2 hours reached the levels shown in Figure 23. These results indicate that residual gas sample contamination during the gas exposure tests is minimal.

3. LOW ENERGY SCANS TO ELUCIDATE LITHIUM REACTIVITY

A series of low energy Auger spectra (1-100 eV) were generated in order to determine the effect of metal-gas exposures on the lithium Auger transition. Figure 24 shows five different Li K-VV scans for: 24a - a typical "clean" lithium metal surface, 24b & 24c - two different nitrogen exposures, 24d - an oxygen exposure, and 24e - a CO_2 exposure. As previously described, prior to each gas exposure the lithium surface was sputtered

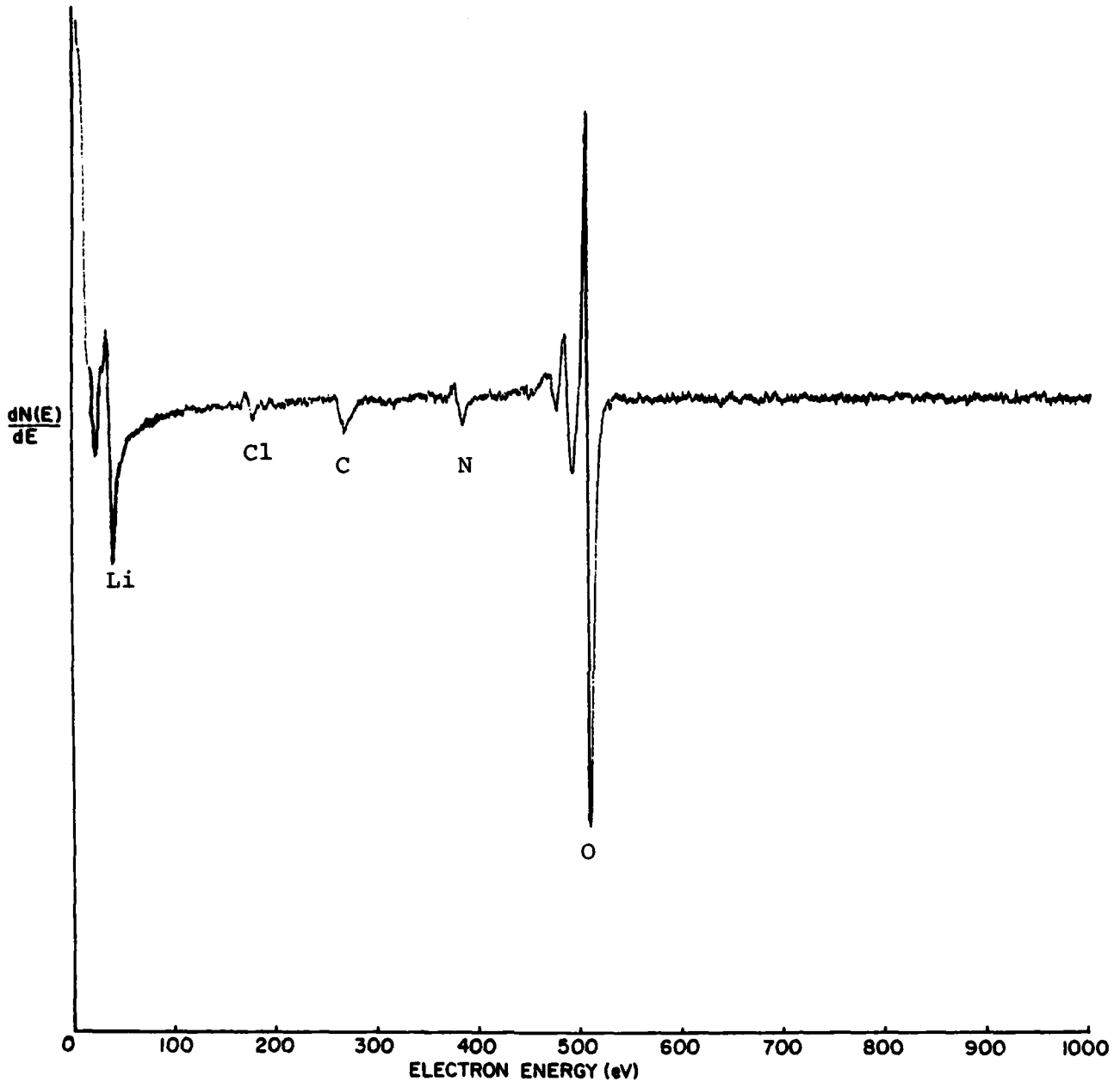

Figure 19. Auger Spectrum of a Lithium Metal Surface As-Cut Under n-Hexane Using the Improved Sample Preparation Technique.

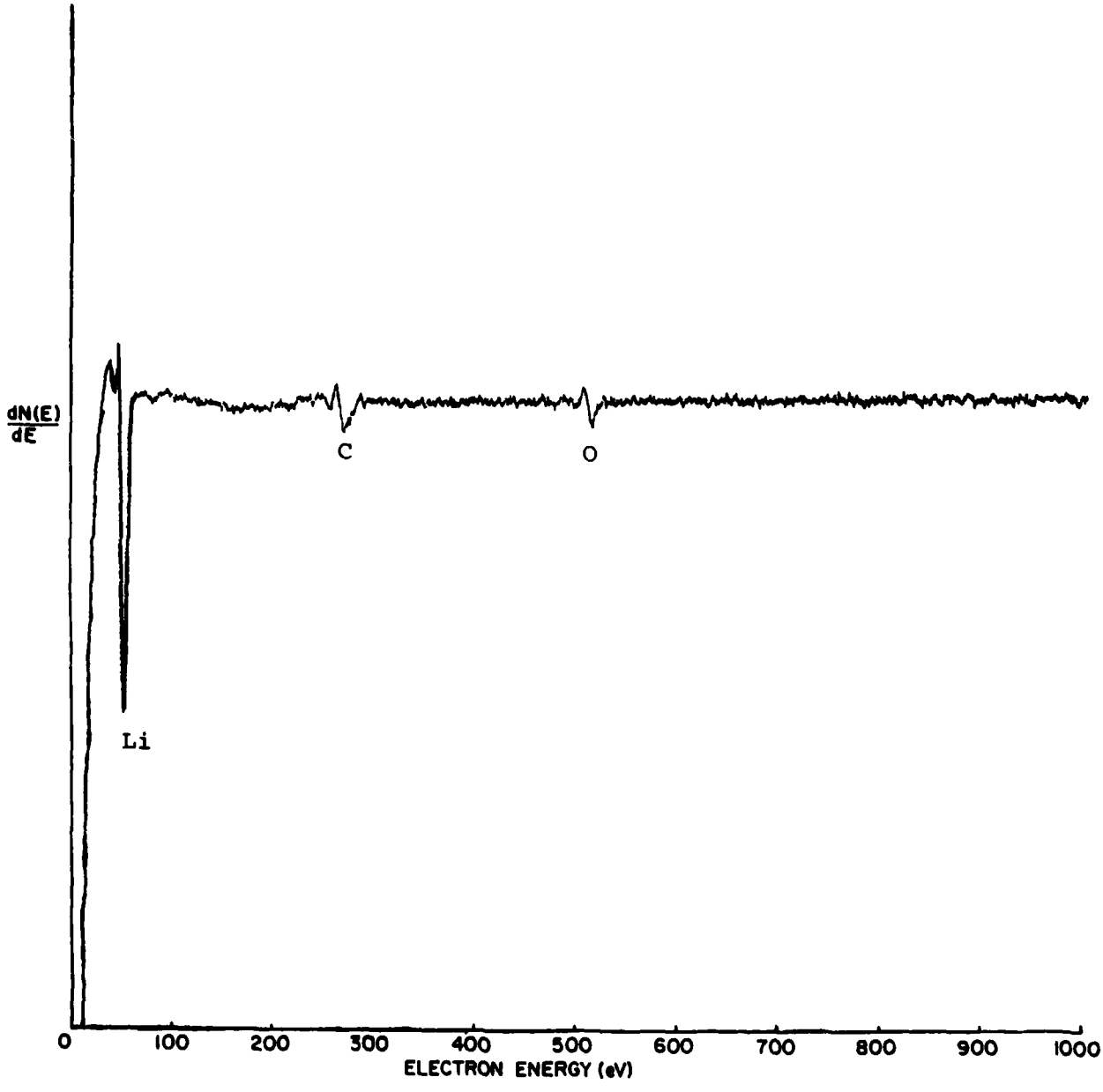

Figure 20. Auger Spectrum of the Lithium Surface Shown in Figure 19 After 5 Minutes of Argon Ion Sputtering.

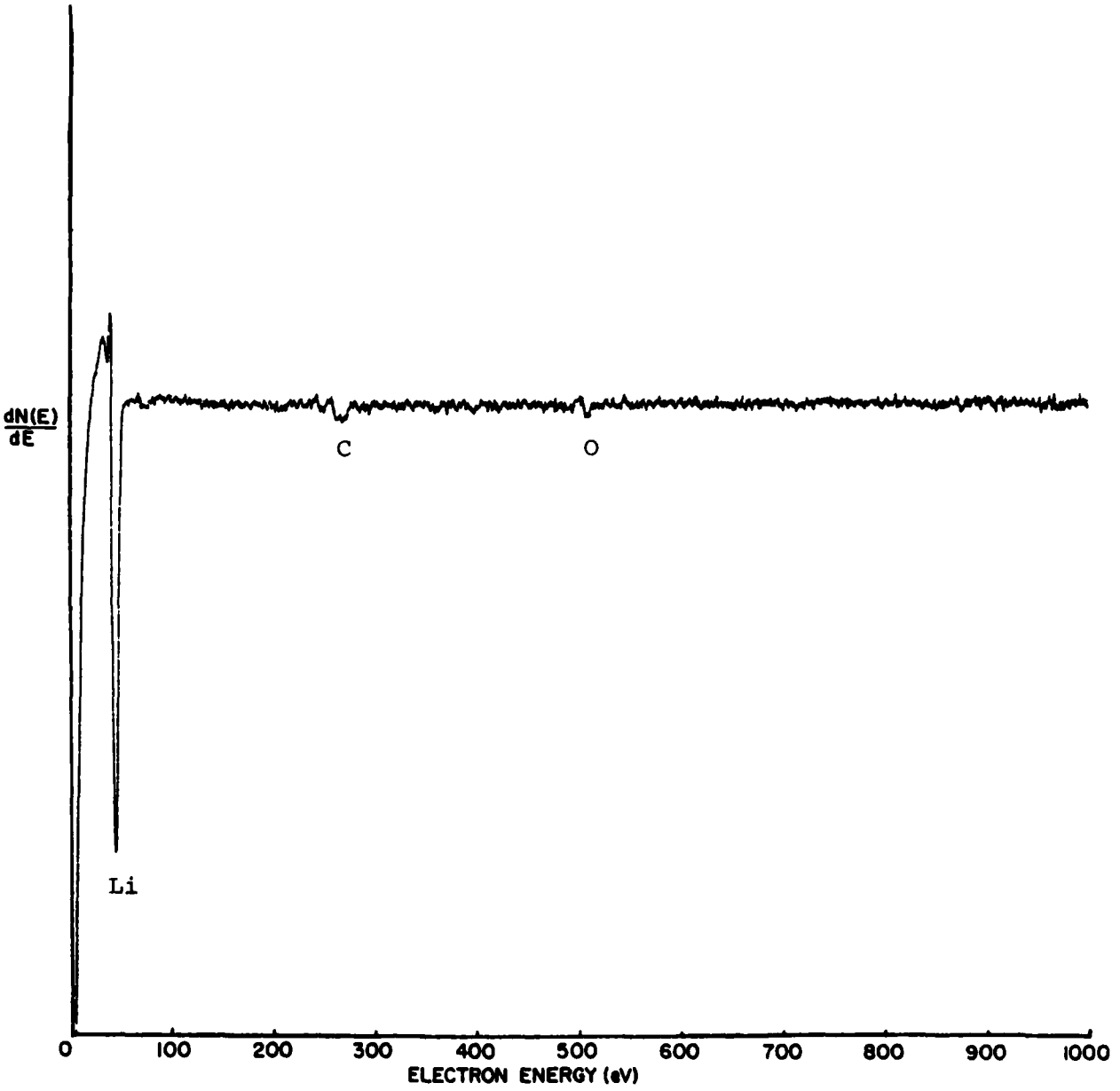

Figure 21. Auger Spectrum of the Lithium Surface Shown in Figure 19 After 17 Minutes of Argon Ion Sputtering.

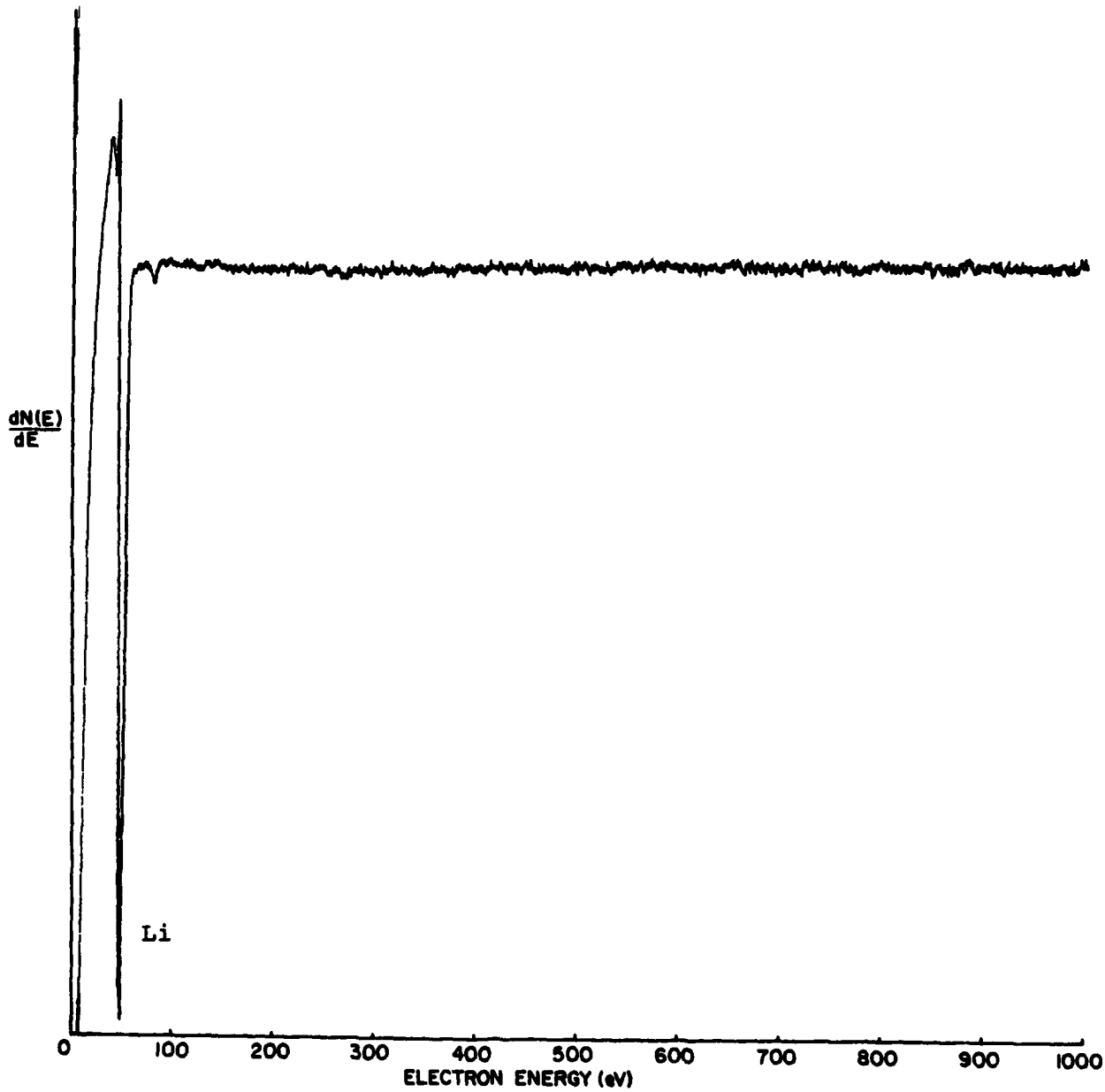

Figure 22. Auger Spectrum of a Clean Lithium Metal Surface Obtained by Repeated Sputtering and Pumping.

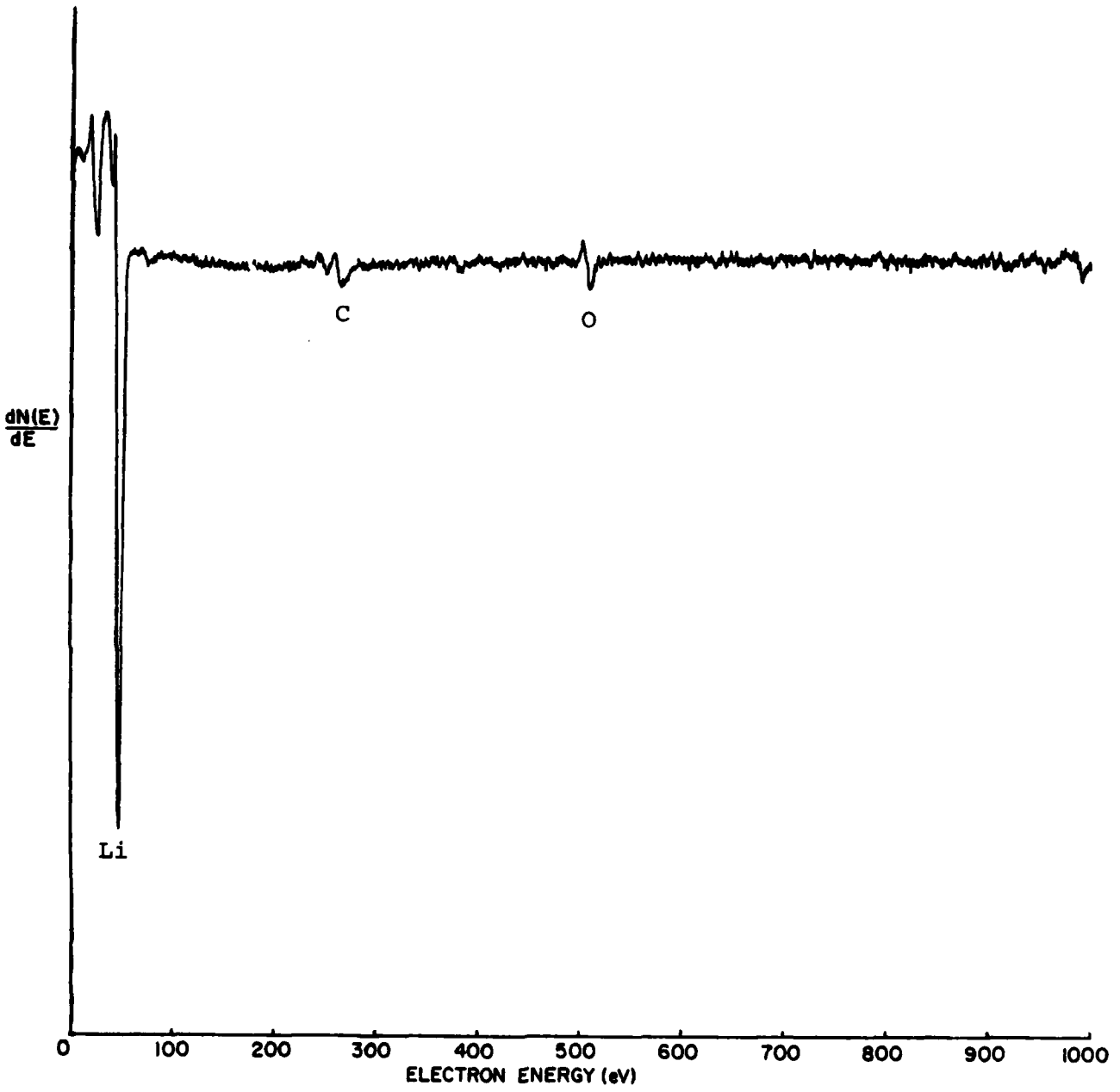

Figure 23. Auger Spectrum Obtained After Allowing a "Clean" Lithium Surface to Age in the Vacuum Chamber for Two Hours.

clean with argon. In each case the resulting "clean" lithium surfaces displayed surface impurity concentrations of less than one atomic percent of oxygen, carbon, and nitrogen. As can be seen from Figure 24a the major Auger peak in the K-VV spectrum of clean lithium metal appears at 51 eV. This is in agreement with previously reported results on lithium metal obtained in this laboratory[34] and elsewhere.[35] A small peak occurs at 82eV and can be easily seen in Figure 22. This is due to the Auger decay of an excited state formed by the excitation of the two 1s electrons. This transition has been observed and reported in the literature,[36] however, no special effort was made to detect it in this study.

All the gas exposure studies resulted in a shift of the 51 eV peak to a lower kinetic energy. For example, the exposure of "clean" lithium metal to oxygen (Figure 24d) resulted in the formation of new structures at 37 and 31 eV. These structures are believed to be lithium oxide. The observable Auger peaks are due to K-VV "cross-over" transitions, that is, transitions which involve K-vacancies in lithium atoms and valence levels, V, predominantly associated with oxygen atoms.

Figures 24b and 24c illustrate the Auger scans generated following nitrogen gas exposures. Note that the main lithium Auger peak has shifted to 50 eV and a new peak has developed at 45 eV. The other peaks are probably due to oxide contamination, but the proper interpretation of this data is difficult. The 50 eV peak is probably due to a chemical shift in the lithium Auger transition following nitrogen adsorption.

4. LITHIUM-THIONYL CHLORIDE EXPOSURE STUDIES USING AES

Samples of lithium metal provided by GTE were either scraped to produce a "clean" surface or left "as received". Samples of both were reacted with thionyl chloride in both liquid and vapor forms.

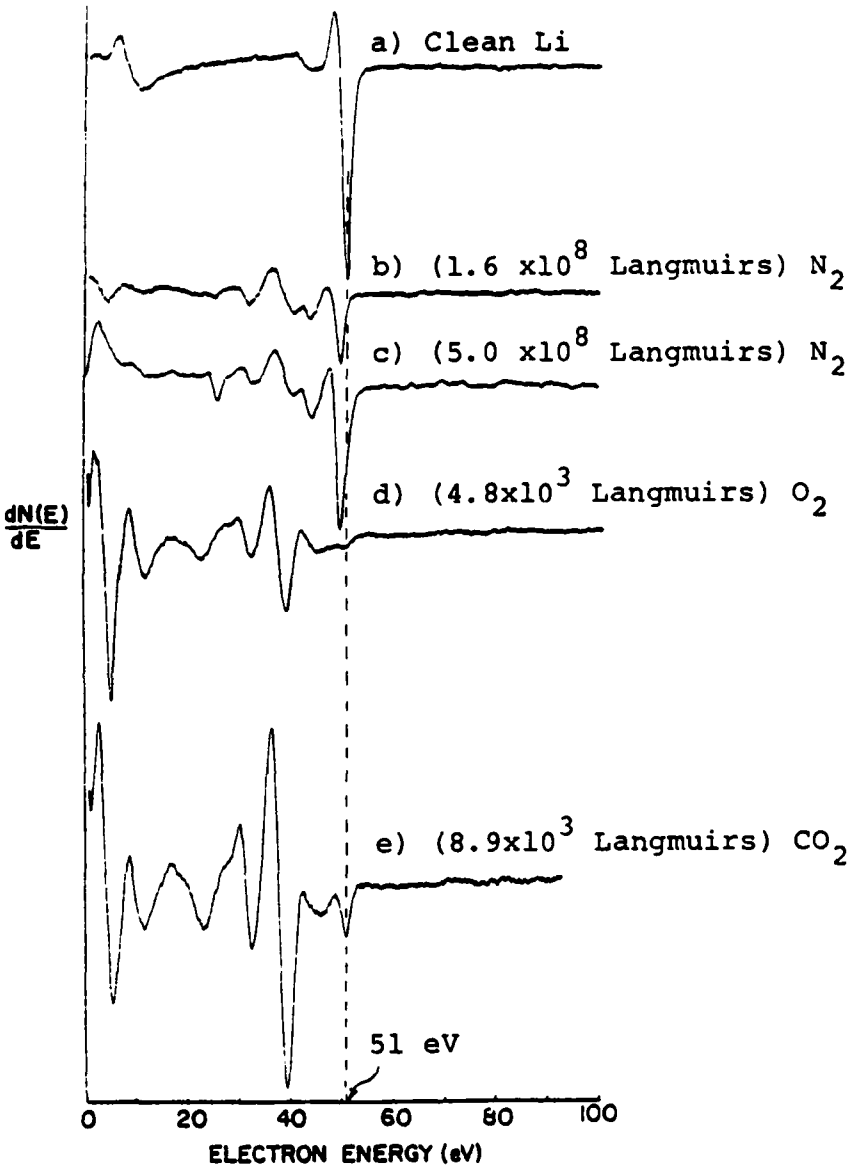

Figure 24. High Resolution Auger Spectra of Lithium; a) Clean Surface; b) Exposed to 1.6×10^8 Langmuirs of nitrogen; c) Exposed to 5.0×10^8 Langmuirs of nitrogen; d) Exposed to 4.8×10^3 Langmuirs of oxygen; e) Exposed to 8.9×10^3 Langmuirs of carbon dioxide.

The results of short and long term exposures of scraped lithium samples to thionyl chloride vapor are shown in Figure 25, while liquid exposures are shown in Figure 26. A short term vapor exposure (Figure 25a) consisted of a five hour exposure in unbaked vials and unbaked Auger chamber, whereas a long term exposure (Figure 25b) was for 11 days in baked vials and baked Auger chamber. Comparison of these two spectra shows an increase in chlorine but a marked decrease in sulfur, carbon, and oxygen with increased exposure time. Careful examination of Figure 25b indicates that two lithium peaks are present. The peak at higher kinetic energy corresponds to lithium metal while the lower energy peak represents the +1 oxidation state. A comparison of time exposures of lithium to $SOCl_2$ in Figure 25a and 25b shows that the surface is cleansed of sulfur, carbon, and oxygen leaving a very thin passivation layer of lithium chloride as exposure times increase. The liquid exposure data presented in Figure 26 shows the same result. Profiling data, which will be discussed later, supports this model since carbon and oxygen decrease throughout the profile. If the passivation layer is thin, less than 5 nm, the detection of the metal peak through the passivation layer is a possibility.

XPS data, presented later, shows the presence of lithium hydroxide on the surface of freshly cut lithium. Upon exposure to both vapor and liquid $SOCl_2$, the formation of the passivating lithium chloride layer could proceed as follows:

$$LiOH + SOCl_2 \rightarrow LiCl + HCl\uparrow + SO_2\uparrow$$

This reaction would support the cleansing model since all but one reaction product is gaseous and could escape the surface. Confirmation of this reaction could be obtained using GC mass spectroscopy. Before a definite conclusion is made on this passivating model a careful study of electron beam effects on the passivation layer would have to be made to rule out electron beam desorption as the mechanism by which lithium metal is being formed.

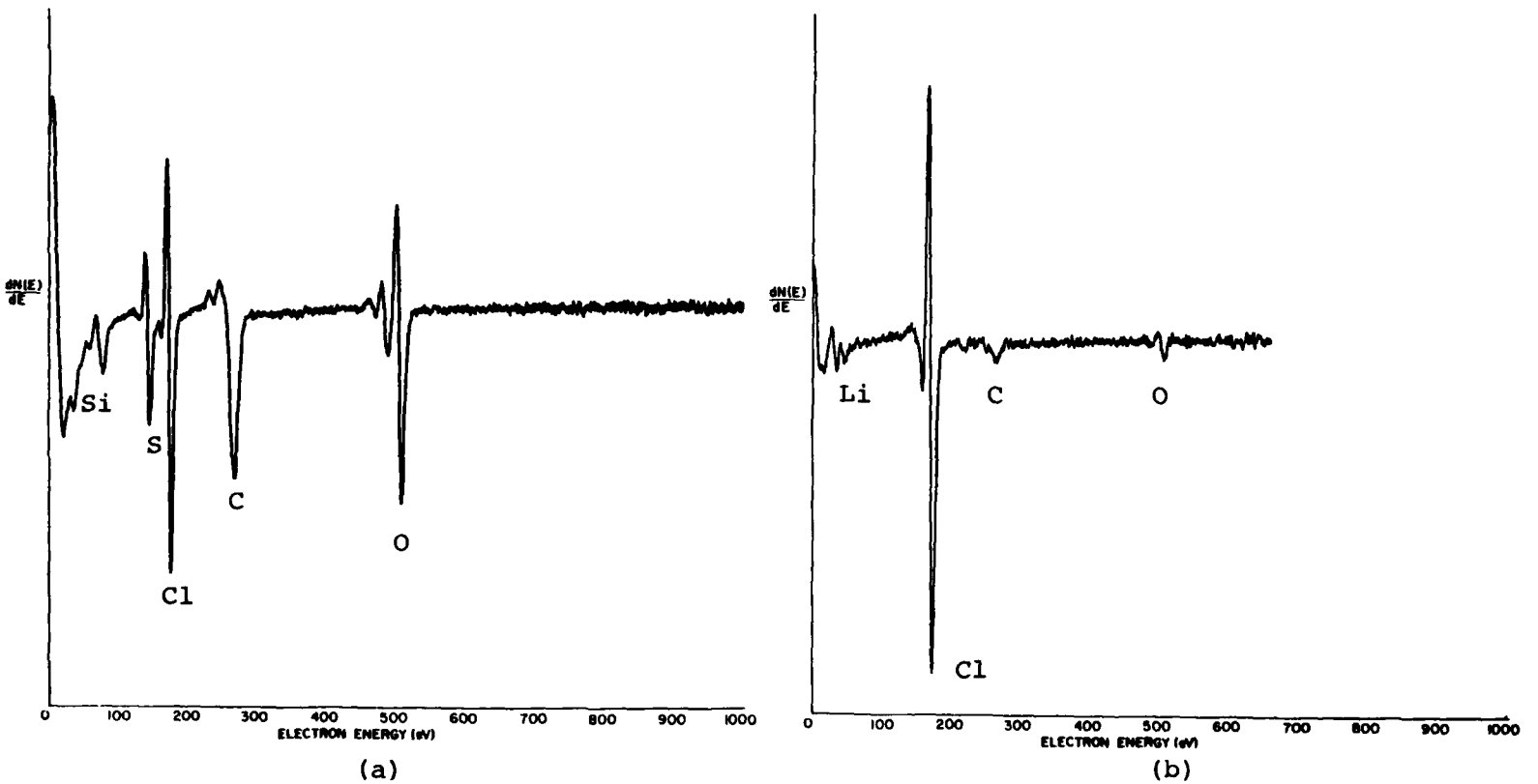

Figure 25. Auger Spectra of a Typical Scraped Lithium Surface (GTE) Exposed to Thionyl Chloride Vapor: (a) Five Hour Exposure in Unbaked Vials and Unbaked Sample Chamber, (b) Eleven Day Exposure in Baked Vials and Baked Sample Chamber.

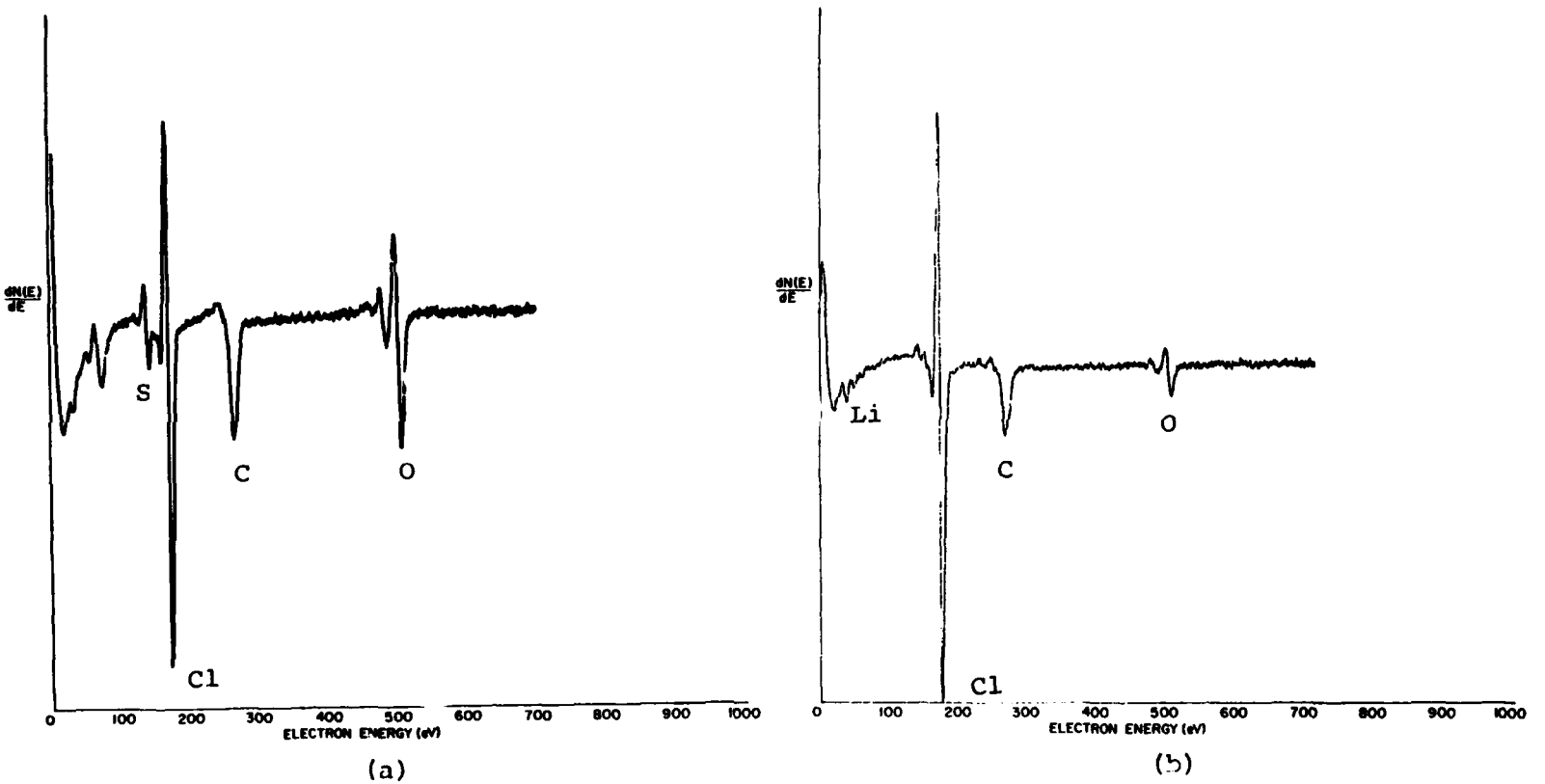

Figure 26. Auger Spectra of a Typical Scraped Lithium Surface (GTE) Exposed to Thionyl Chloride Liquid: a) Five Hour Exposure in Unbaked Vials and Unbaked Sample Charber, b) Eleven Day Exposure in Baked Vials and Baked Sample Chamber.

Residual gas analysis in ultrahigh vacuum systems generally shows the presence of water vapor as a major constituent even at 10^{-9} Torr. The adherence of water vapor to metal and glass surfaces is a well known phenomenon. The effect of baked storage vials for lithium samples and of baking the Auger ultrahigh vacuum chamber has not yet been determined and experiments are now being designed to elucidate these effects. By reducing the amount of water vapor clean lithium surfaces can interact with, more metallic lithium should remain on the surface.

Finally, Figure 27 shows AES spectra of an "as received" lithium sample exposed to both liquid (Figure 27a) and vapor (Figure 27b) $SOCl_2$ for 11 days. The spectra are similar indicating that the passivation reaction has gone to completion during this long term exposure.

It should be noted that the spectrum of the "as-received" lithium surface exposed to $SOCl_2$ vapor (Figure 27b) is quite similar to the spectrum of the scraped lithium surface exposed to $SOCl_2$ vapor (Figure 25b). In both cases, two lithium peaks are detected implying that the passivation process is time related and largely independent of surface preparation.

Profile Experiments

Figures 28 and 29 show profiling data for unscraped lithium exposed to thionyl chloride liquid and vapor, respectively. The profiling curves for the scraped lithium samples exposed to thionyl chloride liquid and vapor, respectively, are presented in Figures 30 and 31. These depth profiles were generated by sputtering with 3kV argon ions. The sputtering rate for lithium chloride under these conditions is unknown; however, the corresponding sputtering rate on copper under these conditions has been measured to be 0.3 nm/sec. The profiles of the scraped samples indicate that the lithium chloride layer is thin, probably less than 10 nm. Although these profiles indicate the chloride

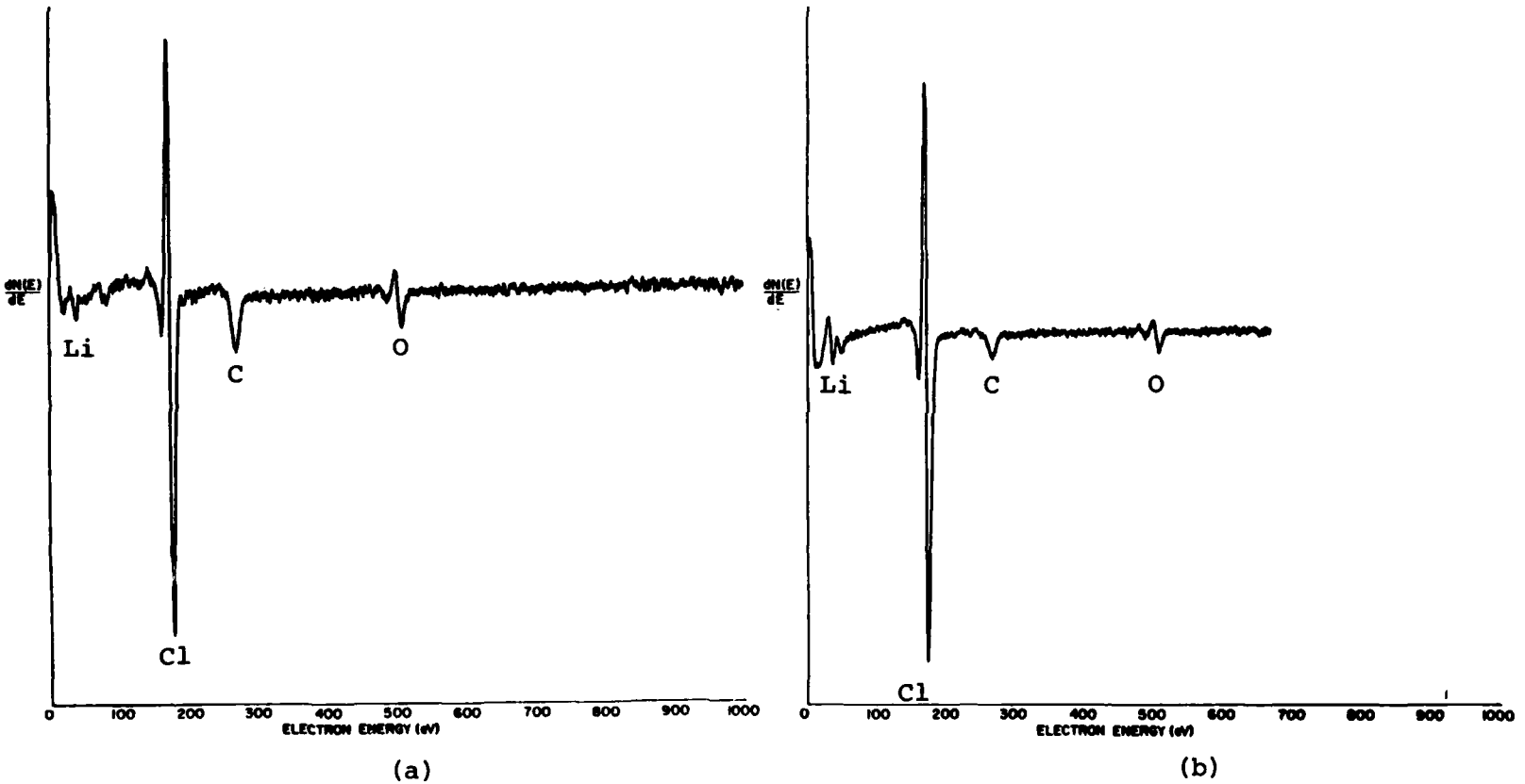

Figure 27. Auger Spectra of a Typical Lithium Surface "As Received" From GTE: (a) Eleven Day Exposure to Liquid Thionyl Chloride in Baked Vials and Baked Sample Chamber, (b) Eleven Day Exposure to Vapor Thionyl Chloride in Baked Vials and Baked Sample Chamber.

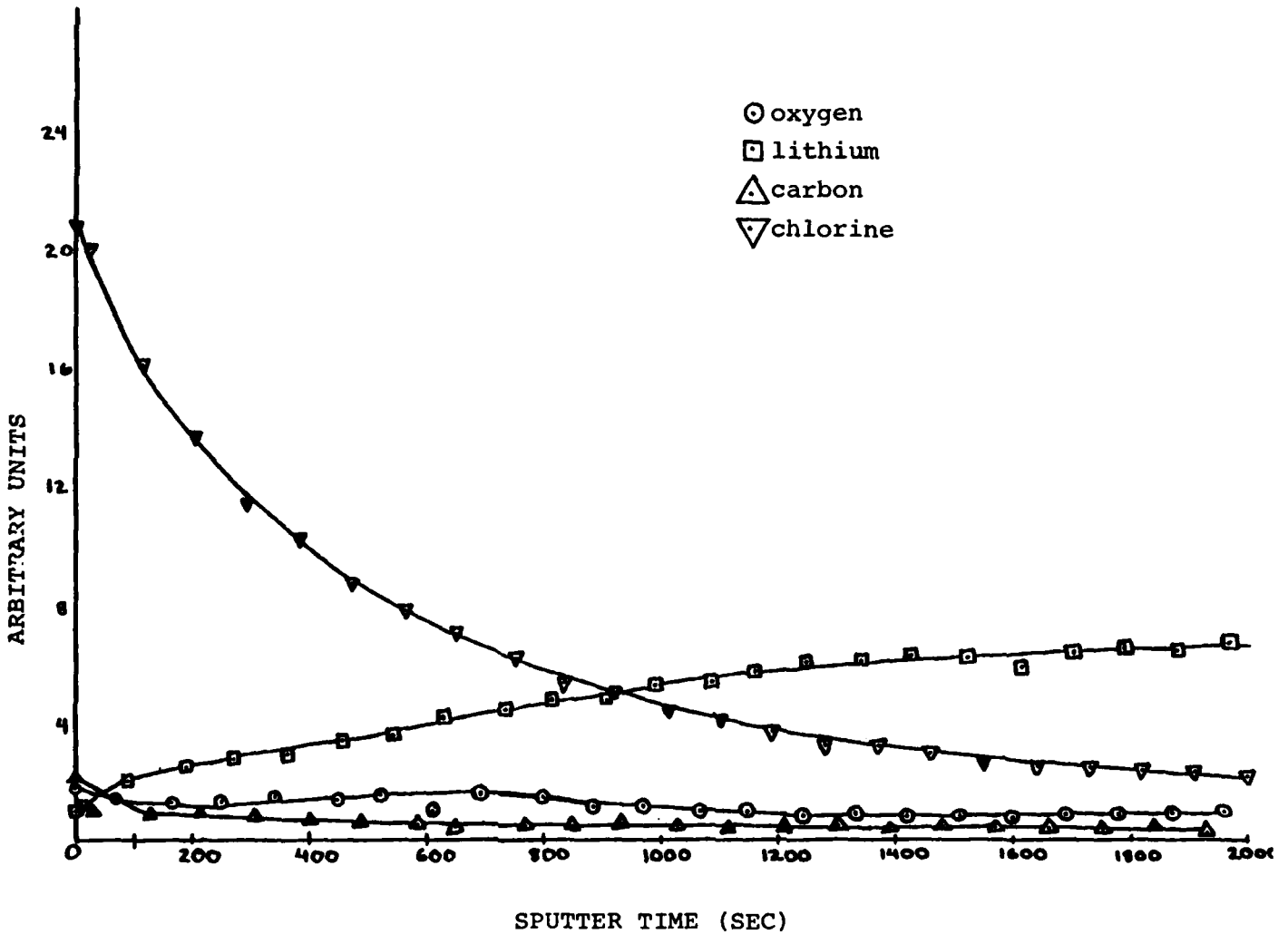

Figure 28. Auger Profile of an "As Received" GTE Lithium Surface Exposed to Liquid Thionyl Chloride Eleven Days.

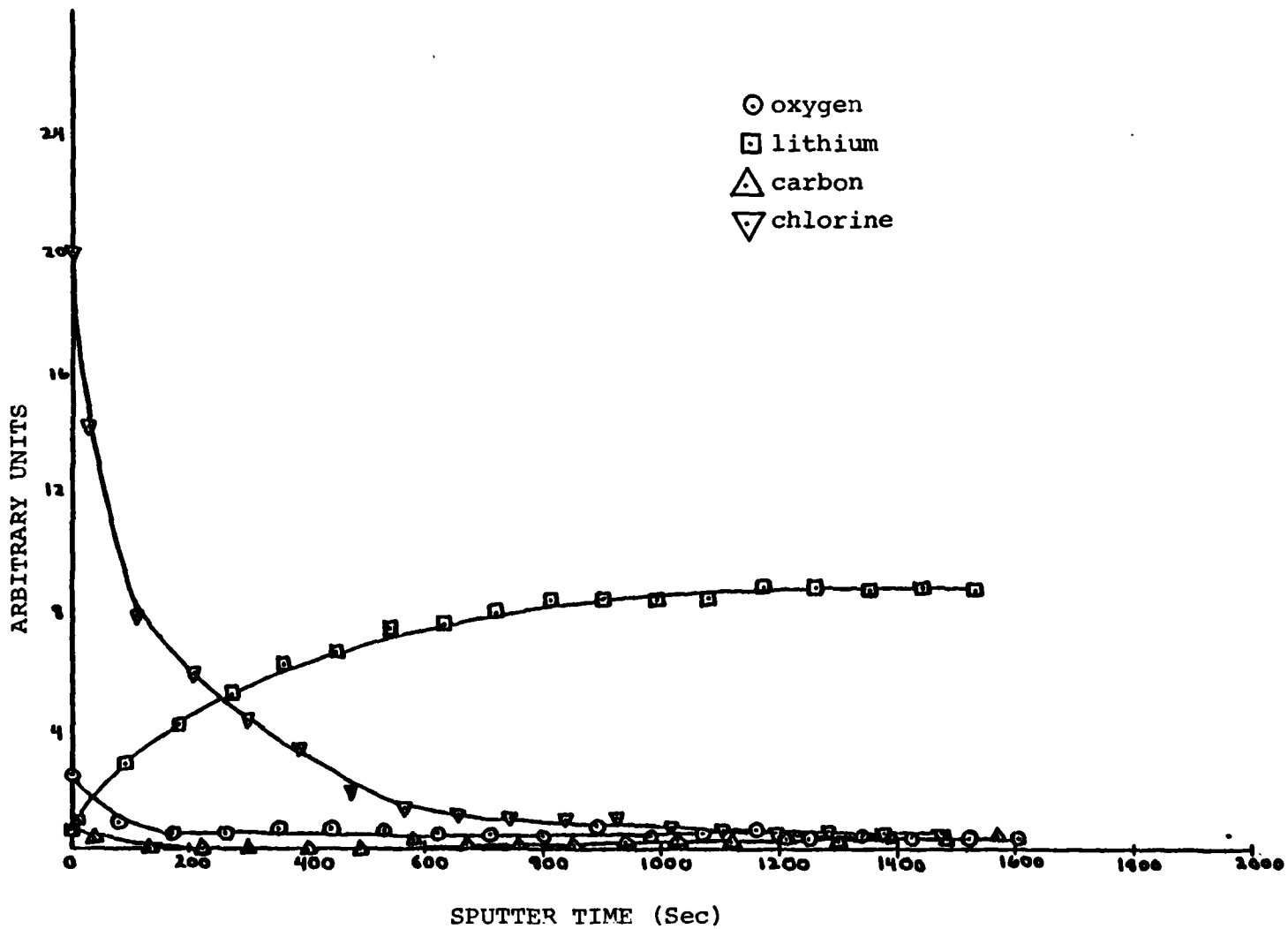

Figure 29. Auger Profile of an "As Received" GTE Lithium Surface Exposed to Thionyl Chloride Vapor Eleven Days.

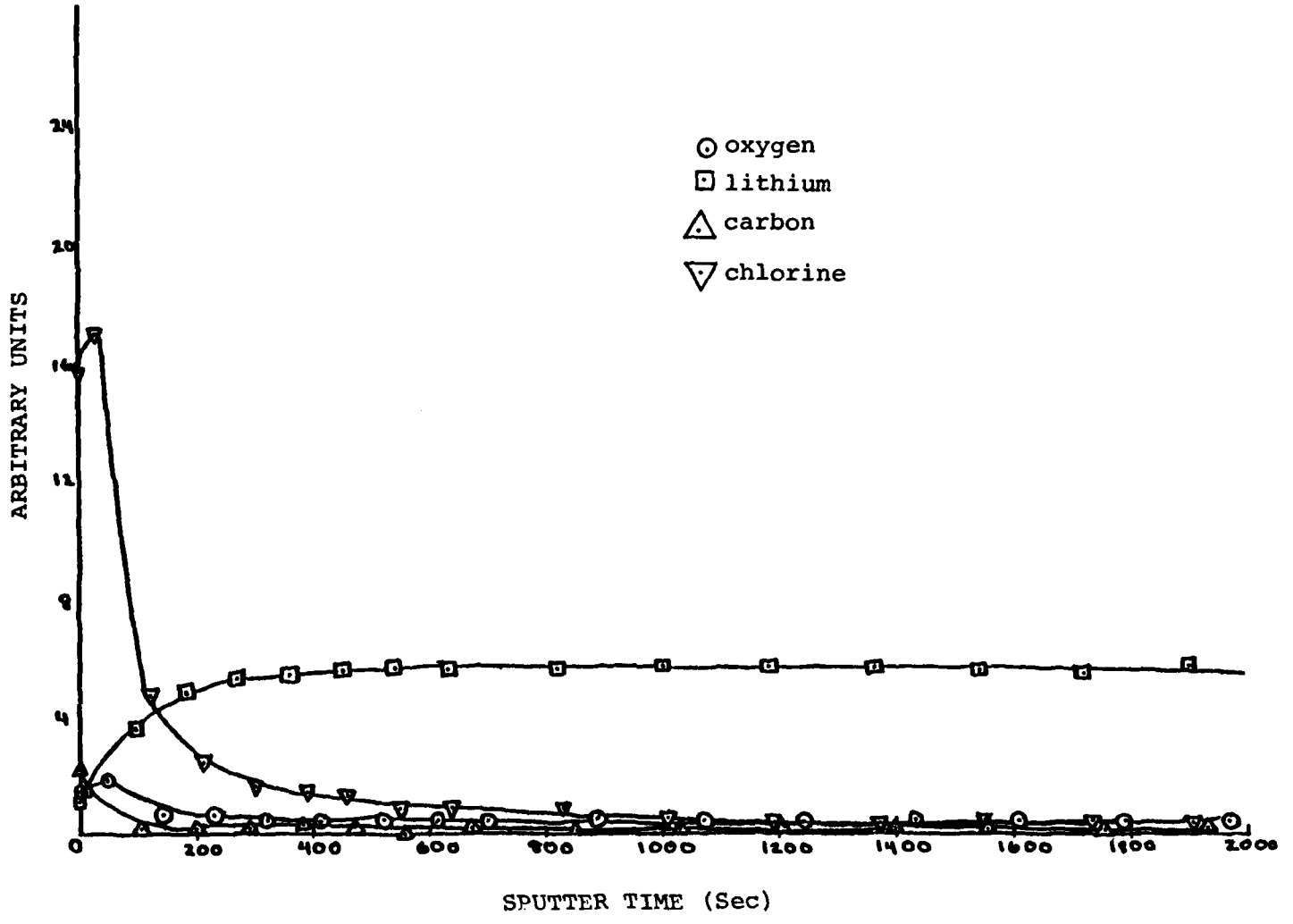

Figure 30. Auger Profile of a Scraped GTE Lithium Surface Exposed to Liquid Thionyl Chloride Eleven Days.

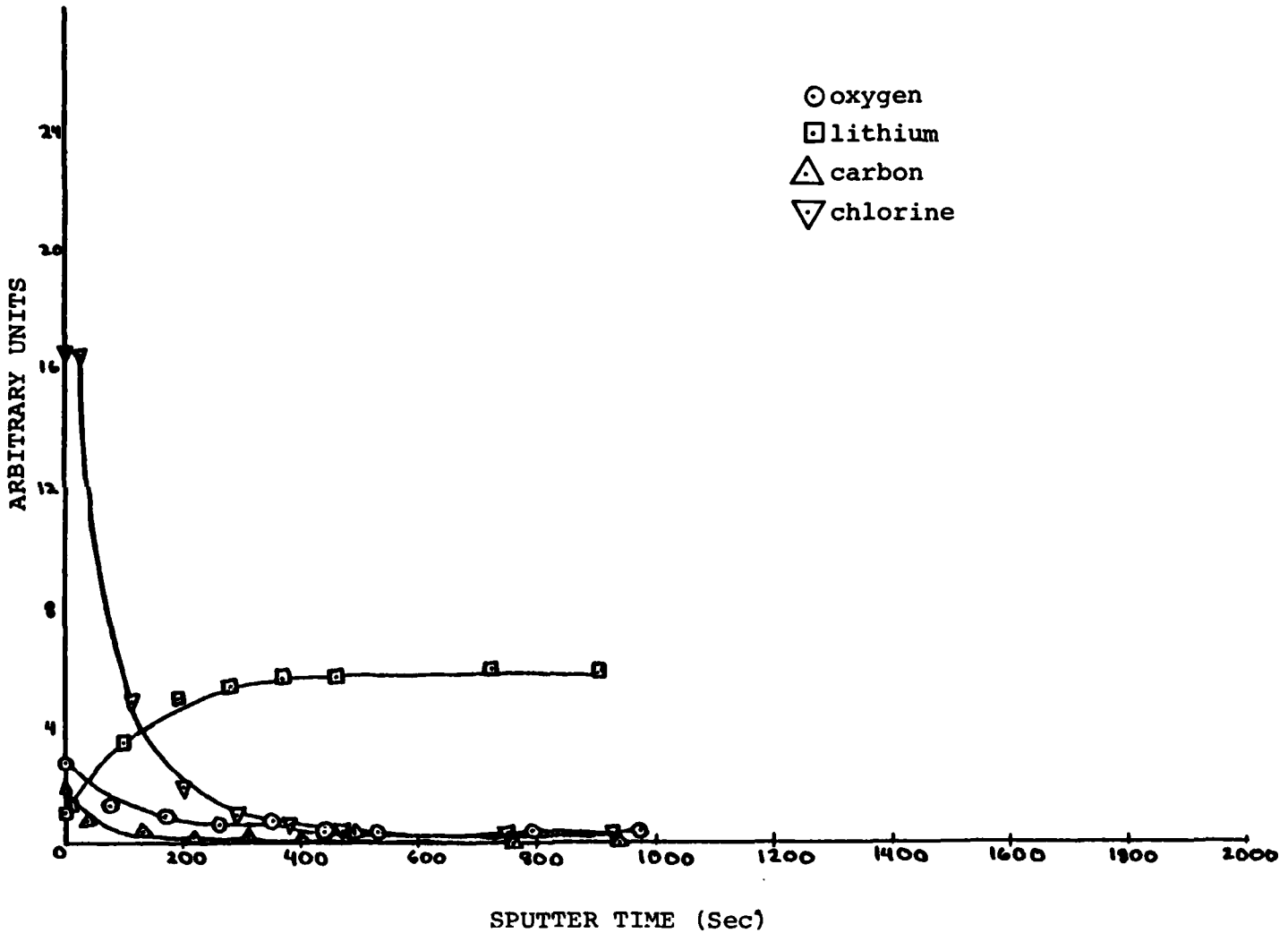

Figure 31. Auger Profile of a Scraped GTE Lithium Surface Exposed to Thionyl Chloride Vapor Eleven Days.

passivation layer is thicker on the "as received" samples than on the scraped samples, the difference in surface roughness may account for these sputtering differences. Since visual inspection of all the lithium samples used in this study showed that all scraped samples were generally smoother than the unscraped samples, depth profile broadening due to surface roughness is suspected.

5. BLACK SPOT FORMATION

An as-received, argon stored ribbon sample of lithium was exposed overnight in a container of dry nitrogen gas. Within 12 hours, black nodules approximately 0.3 cm in diameter were observed randomly across the ribbon surface. Several small samples were then cut from the ribbon under n-hexane and analyzed.

AES spectra of a nodule and the surrounding region are shown in Figures 32 and 33 respectively. After overnight exposure to nitrogen the spectrum shown in Figure 34 was obtained showing a significant enrichment of nitrogen indicating that the black spotted area is a lithium nitride or oxynitride type material. The sputtering data in Figure 35 shows the increase in intensity of the nitrogen Auger signal and the decrease in intensity of C and O Auger signals as the spot was ion milled.

High resolution spectra of the spotted and off-spot areas were taken of the lithium and oxygen Auger peaks which are shown in Figure 36. These results are consistent with the results discussed above and indicate the black spotted region is a nitride or an oxynitride.

The circular symmetry and hemispherical shape of the spots from the surface inward indicate the presence of an active surface site which provides a nucleating site after which rapid growth after exposure occurs. The origin or nature of this site has not been established. This explanation is consistent

with the slow reaction rate of lithium with nitrogen as determined in these experiments.

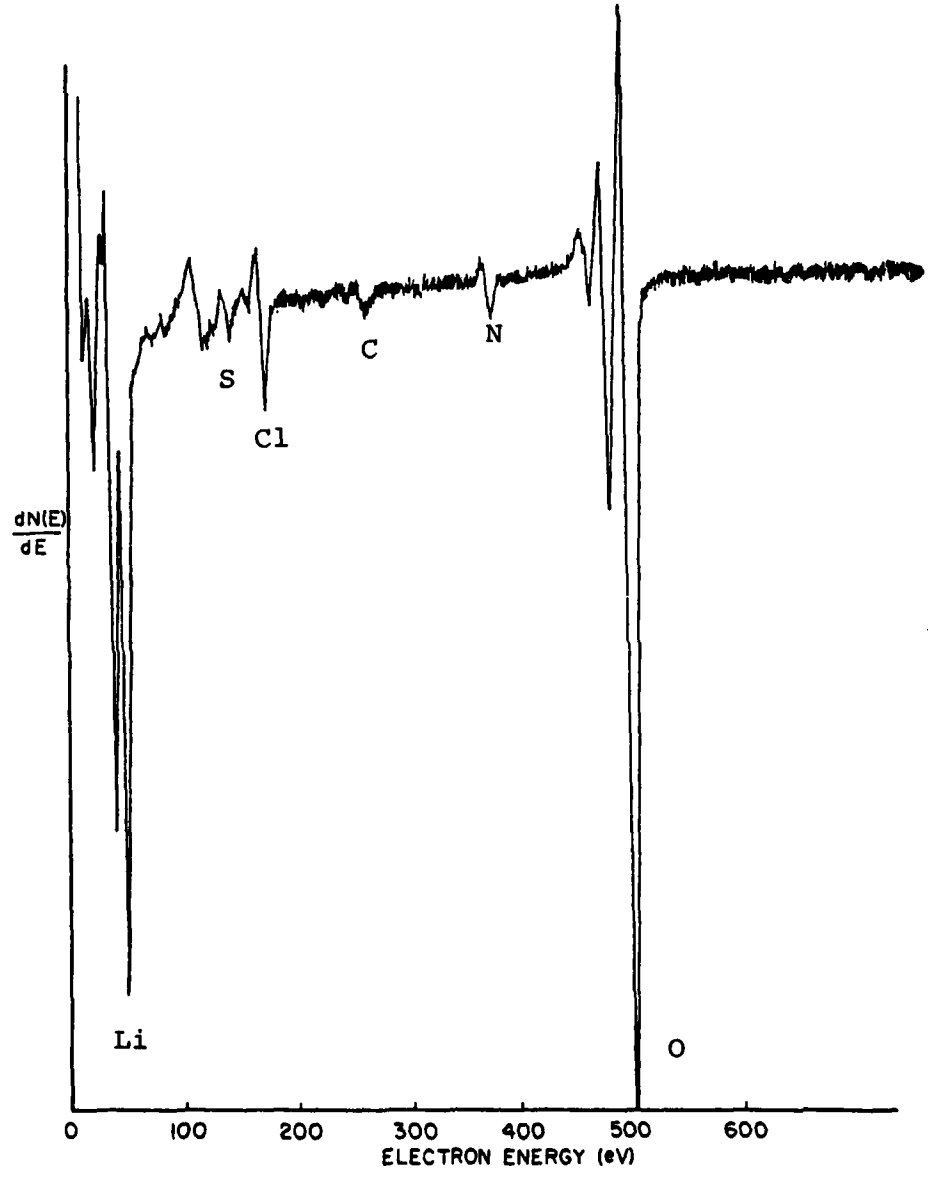

Figure 32. Auger Spectrum of a Lithium Surface During the Early Growth Stages of a Black Spot.

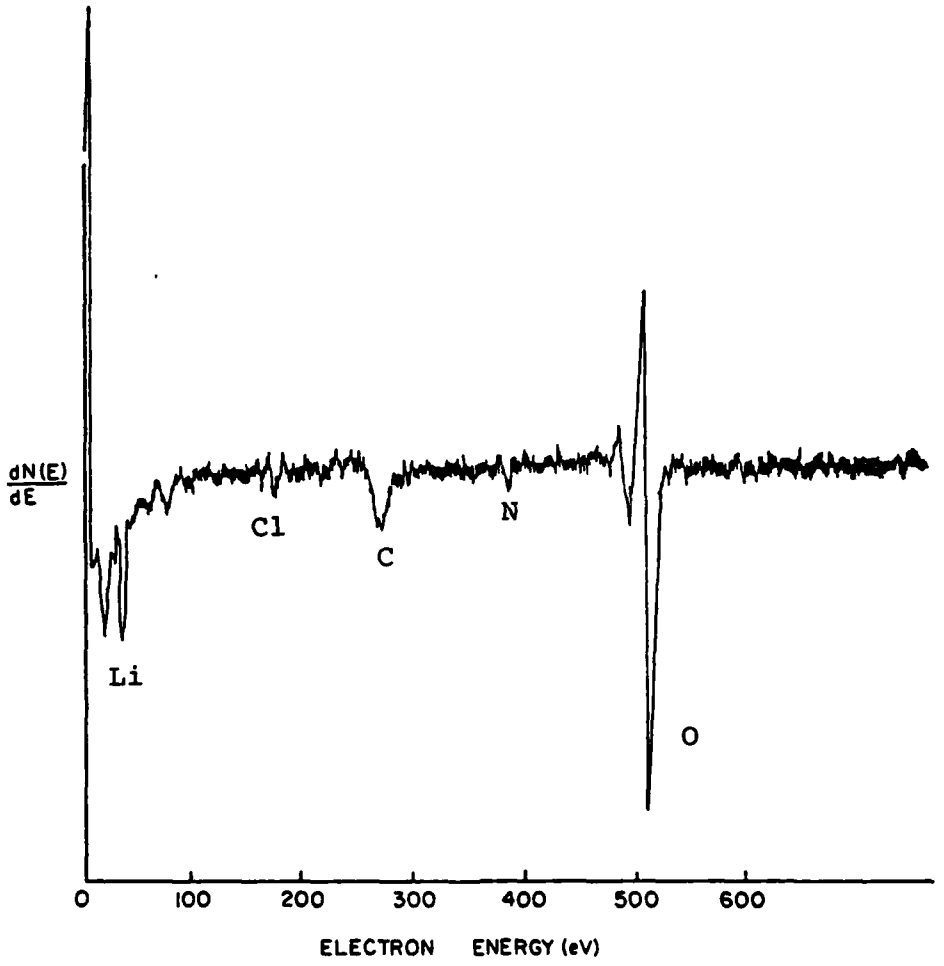

Figure 33. Auger Spectrum of a Lithium Surface Adjacent to a Black Spot.

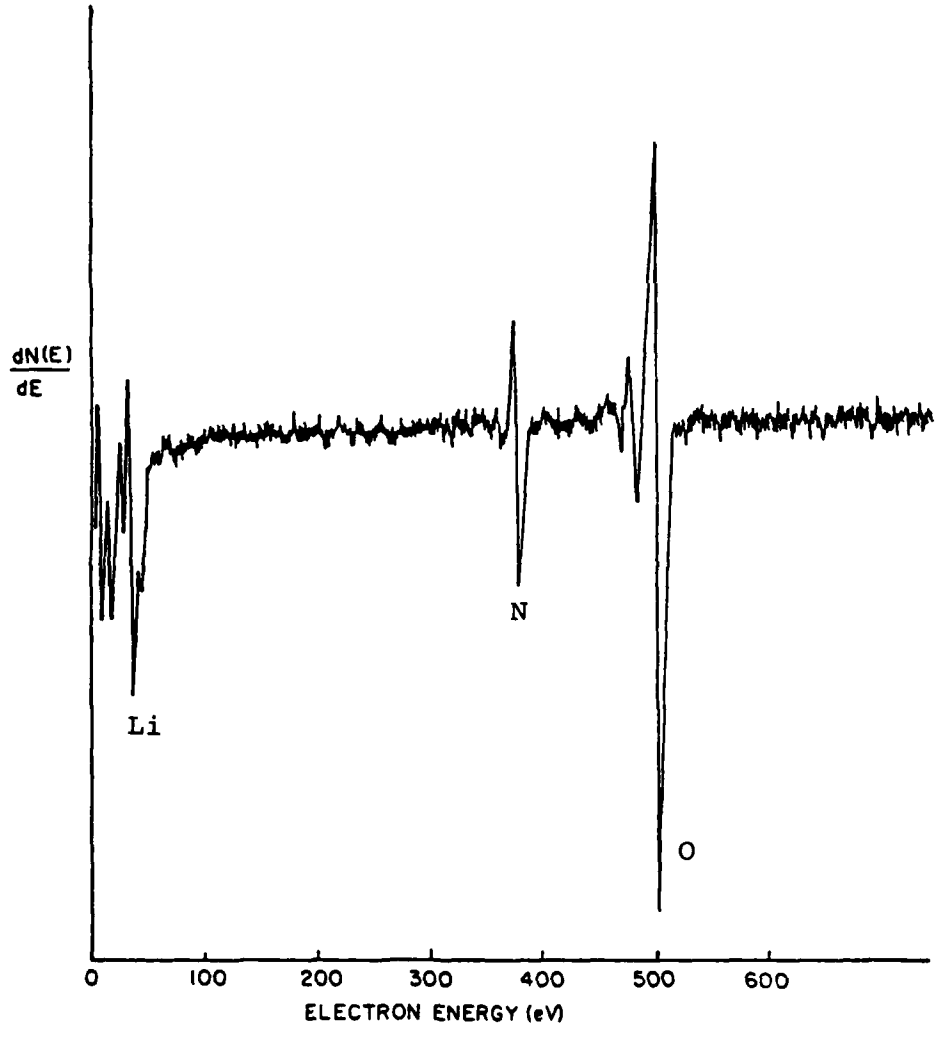

Figure 34. Auger Spectrum of Black Spot on a Lithium Surface After an Overnight Exposure to Nitrogen.

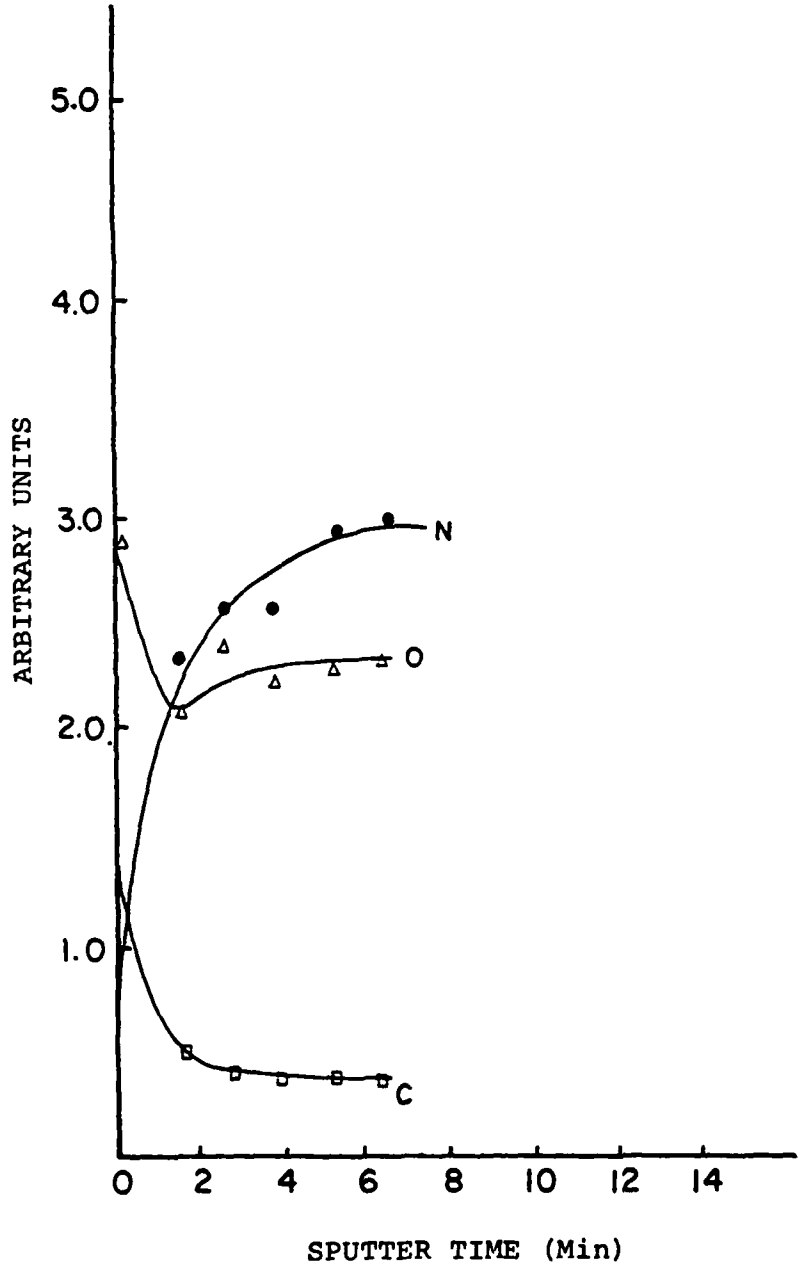

Figure 35. Auger Depth Profile of a Black Spot Created After Overnight Exposure to Nitrogen.

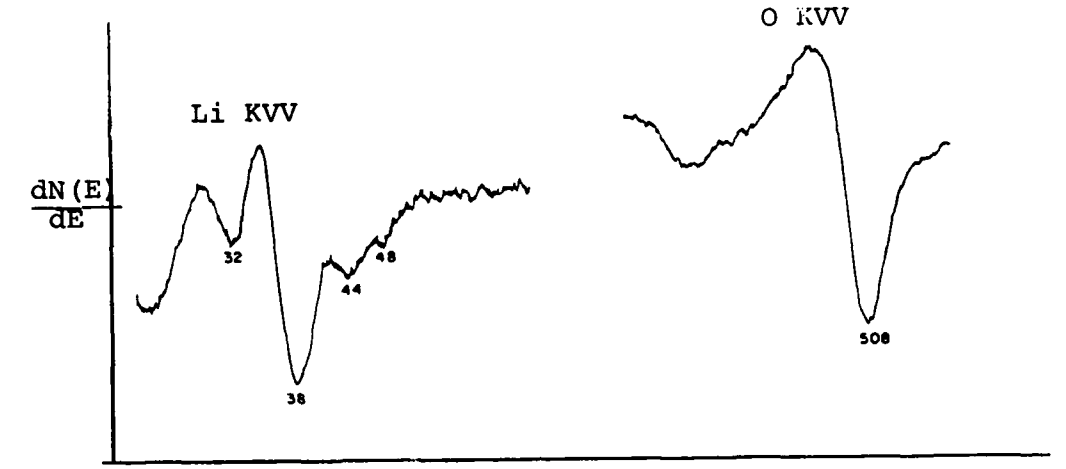

Auger Energy (eV)

(a) Unspotted Region

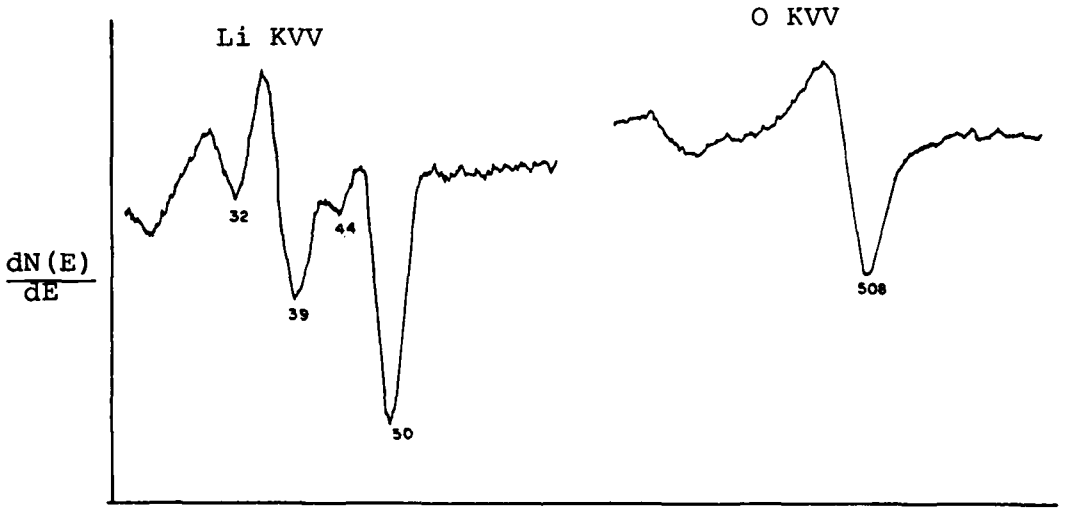

Auger Energy (eV)

(b) Spotted Region

Figure 36. High Resolution Auger Spectra of Lithium and Oxygen: a) Unspotted Region, b) Spotted Region.

SECTION 5
XPS STUDIES OF LITHIUM

Lithium metal, freshly cut in our dry box was mounted in the transfer chamber and inserted into the XPS instrument for analysis. The samples were cut in a helium ambient environment in which the water content was recorded at 1.25 ppm. The time required to mount a freshly cut sample and seal it into the transfer chamber was approximately three minutes. After transfer, the XPS insertion chamber was immediately evacuated to 10^{-8} Torr and baked before the gate valve of the transfer chamber was opened. A typical overall XPS scan of high purity lithium supplied by Foote Mineral Company prepared in this manner is given in Figure 37. The elements found to be present in the overall scan are: oxygen (43 percent), lithium (28 percent), carbon (27 percent) and chlorine (2 percent). These results ignore any contribution from hydrogen, since the bonded hydrogen 1s electron in hydrogen molecules is difficult to observe with XPS. Three additional overall scans were made on Foote lithium surfaces freshly cut in the helium drybox. The results were found to be essentially the same with the only differences being in the amount of carbon contamination. The presence of a trace amount of silicon was noted in some spectra. Since the lithium metal was cut with a razor blade, the presence of silicon could be due to a silicone surfactant being transferred from the blade to the metal. To prevent this problem a surgical steel scalpel is now being used.

Figure 38 shows the O 1s XPS scans obtained in our laboratory from freshly cut lithium following insertion into the XPS sytem (Figure 38a), after some argon ion bombardment (Figure 38b) and after further ion bombardment (Figure 38c). The conversion of the hydroxide to oxide under ion bombardment is apparent. These peak assignments to hydroxide and oxide are in agreement with a previous study done on water chemisorption on magnesium metal.[37] With results similar to those shown for the O 1s

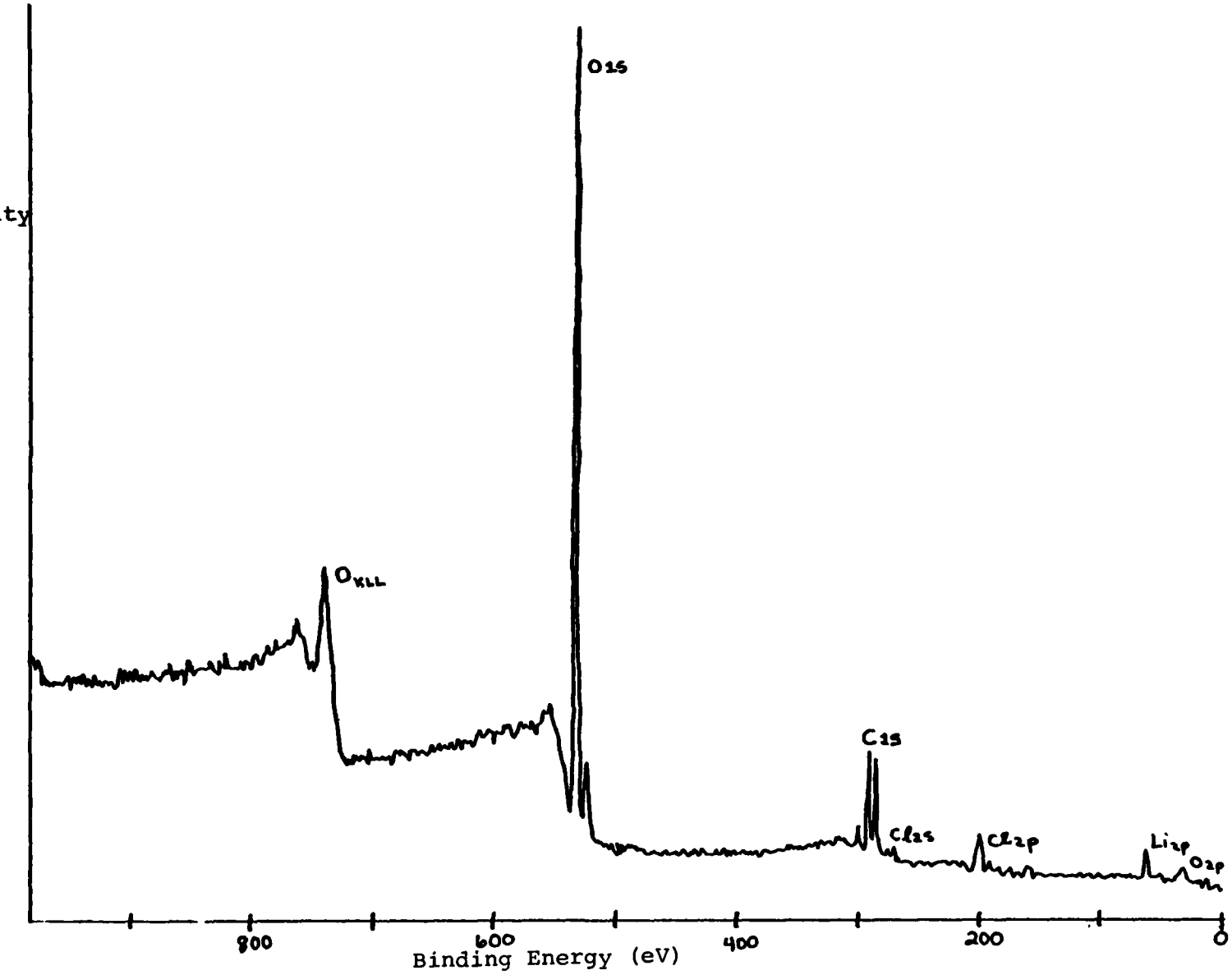

Figure 37. Typical Overall XPS Scan of Foote Mineral Lithium Freshly Cut in Inert Atmosphere.

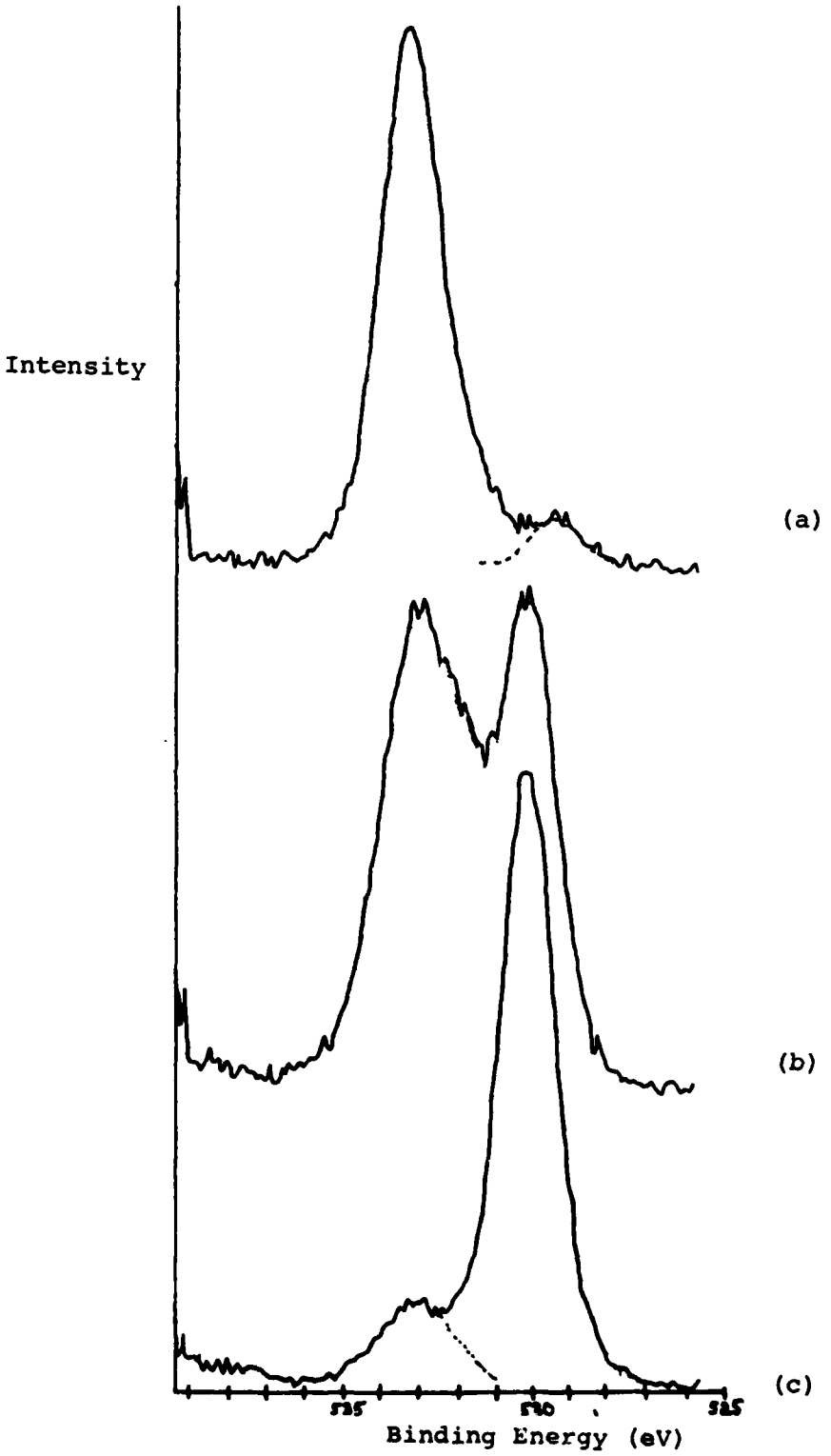

Figure 38. High Resolution O 1s XPS Spectra of: a) Lithium Hydroxide, b) Approximately Equal Amounts of Lithium Hydroxide and Lithium Oxide, and c) Lithium Oxide.

spectrum (Figure 38) a determination of the relative amounts of surface hydroxide and oxide can be made for the lithium anodes obtained from the battery assembly room. We do not observe any detectable chemical shift in the lithium 1s spectrum as a function of hydroxide-oxide mixture. This is to be expected from electronegativity consideration since in both lithium oxide and hydroxide the lithium is bound to oxygen.[38]

SECTION 6
SUMMARY AND CONCLUSIONS

Results in this laboratory during the past year have been significant and positive. We have demonstrated the ability to control environmental conditions, to transfer samples from these controlled environments to spectrometers without serious contamination, and to prepare "clean" lithium metal surfaces.

We have developed the necessary hardware to pursue detailed XPS and AES studies of the interaction of gases with lithium metal surfaces, and on the basis of AES results believe reactivity of certain gases with lithium decreases in the series $CO_2 > O_2 > H_2O > N_2$. Black spots, observed on some GTE lithium anode samples, have been formed by exposing lithium to nitrogen. These spots are most probably a nitride or an oxynitride.

Using AES, the reaction of lithium with thionyl chloride has been found to produce a thin layer of lithium chloride as a primary reaction product. It has been shown that carbon, sulfur, and oxygen levels decrease as the passivation process proceeds. Depth profiles of passivated lithium surfaces show that the chloride passivation layer is thin, probably less than 10 nm and that carbon and oxygen are removed from the surface rather than being covered over by lithium chloride.

We have demonstrated, using XPS, the ability to observe relative concentration differences of lithium oxide and lithium hydroxide on the surface of freshly cut lithium.

REFERENCES

1. Lattimer, W. M., "The Oxidation States of the Elements and Their Potentials on Aqueous Solutions," 2nd Ed., Prentice Hall, Inc., Englewood Cliffs, N.J. (1952).
2. Jasinski, R., "High Energy Batteries," Chap. 4, Plenum Press, New York (1967).
3. Klaus, H. M., Braeuer, M., and Harvey, J. A., "Status Report on Organic Electrolyte High Energy Density Batteries," ECOM, May 1967.
4. Gabano, J. P., Gerbies, G., and Laurent, J. F., "High Energy Cells with a Lithium Electrode," Proc. 23rd Annual Power Sources Conference, pp. 80-83, May 1969.
5. Knapp, H. R., ECOM TR-2632, October 1965.
6. Hunger, H. F., and Heymach, G. J., J. Electrochem. Soc., 120, 1161 (1973).
7. Dampier, F. W., J. Electrochem. Soc., 121, 656 (1974).
8. Dey, A. N., "Lithium Metal Oxide Organic Electrolyte Primary Batteries," Abstract #54, Meeting of Electrochemical Society, October 1973, Boston, Mass.
9. Gabano, J. P., Yamel, Y., and Gornis, J. P., Abstract #55, Ibid.
10. Campanella, L., and Pistoria, G., J. Electrochem. Soc., 118, 1905 (1975).
11. Jasinski, R., Gaines, L., Hansen, G., and Carroll, S., "Lithium Nickel Sulfide Batteries," Proc. 24th Power Sources Symposium, pp. 98-100, May 1970.
12. Gabano, J. P., Gerbier, G., and Laurent, J. F., "High Energy Cells with a Lithium Electrode," Proc. 23rd Annual Power Source Conference, pp. 80-83, May 1969.
13. Fiordiponti, P., Pistoia, G., and Tempetni, C., J. Electrochem. Soc., 125, 14 (1978).

14. Rudorf, W., "Graphite Intercalation Compounds," in Advances in Inorganic Chemistry and Radiochemistry, 1, ed. by J. Embers and A. G. Sharpe, Academic Press, Inc., New York (1959).
15. Braeuer, K., "Feasibility Study of the Lithium/CxF Primary Cell," Research and Development Technical Report ECOM-3322, August 1970.
16. Watanabe, N., and Eijima, T., Abstract #41, Fall Meeting of the Electrochemical Society, October 1971, Cleveland, Ohio.
17. Brooks, E., "Organic Electrolyte Batteries," Proceedings Seventh Intersociety Energy Conversion Engineering Conference, September 1972.
18. Wilburn, N. T., "Organic Electrolyte Batteries," Proceedings 25th Power Sources Symposium, pp. 3-5, May 1972.
19. Maricle, D. L., and Mohns, J. P., U.S. Patent 3,567,515, March 1971.
20. Behl, W. K., Choistopulos, J. A., Ramirez, M., and Gilman, S., "Lithium Inorganic Electrolyte Cells Utilizing Solvent Reduction," Abstract #59, Meeting of the Electrochemical Society, October 1973, Boston, Mass.
21. Auburn, J. J., Frerich, K. W., Lieberman, S. I., Shah, V. K., and Heller, A., J. Electrochem. Soc., 120, 1613 (1973).
22. Gehl, W., Choistopulos, J., Ramirez, M., and Gilman, S., J. Electrochem. Soc., 120, 1619 (1973).
23. Gilman, S., "An Overview of the Primary Lithium Battery Program," Proceedings 26th Power Sources Symposium.
24. Dey, A. N., "Sealed Primary Lithium-Inorganic Electrolyte Cell," Third Quarterly Report, ECOM-74-0109-3, March 1975.
25. Driscoll, J. R., Holleck, G. L., Taland, D. E., and Brummer, S. B., "Lithium-Inorganic Electrolyte Batteries," Eighth Quarterly Report, ECOM-74-0030-8, January 1976.
26. Dey, A. N., and Schlaikjer, C. R., "The Voltage Delay Problem with the Thionyl Chloride System and Some SEM Studies of Lithium Film Growth," 26th Power Sources Symposium, 26, 47 (1975).

27. Dey, A. N., Electrochemica Acta, 21, 855 (1976).
28. Chua, D. L., Merz, W. C., and Bishop, W. S., "Lithium Passivation in the Thionyl Chloride System," Proceedings 26th Power Sources Symposium.
29. Dey, A. N., "Primary Li/$SOCl_2$ Cells II. Thermal Runaways and Their Prevention in Hermetic D Cells," Proceedings 26th Power Sources Symposium.
30. Brooks, E. S., "Evaluation of Designs for Safe Operation of Lithium Batteries," Proceedings 26th Power Sources Symposium.
31. Private Communication, November 1978.
32. Driscoll, J. R., Holleck, G. L., Toland, D. E., "Reactions in Lithium Thionyl Chloride Cells," Proceedings 26th Power Sources Symposium.
33. Holleck, G. L., Turchan, M. J., and Cogley, D. R., 4th Quarterly Report, Contract DAAB07-74-C-0030 (ECOM), EIC, Inc., January 1975.
34. Froning, M. H., Moddeman, W. E., Wittberg, T. N., and David, D. J., "Non-Aqueous Electrode Research", Interim Technical Report, AFAPL-TR-79-2003, February 1979.
35. R. E. Clausing, D. S. Easton and G. L. Powell, Surface Science, 36, 377 (1973).
36. G. L. Powell, G. E. McGuire, D. S. Easton and R. E. Clausing, Surf. Sci., 46. 345 (1974).
37. J. C. Fuggle, L. M. Watson, and D. J. Fabian, Surface Sci., 49, 61 (1975).
38. K. Siegbahn et al., Nova Acta Reg. Soc., Upsakensis, Ser. IV, 20 (1967) 1.

*U.S.Government Printing Office: 1980 — 657-084/669